

Qudits and high-dimensional quantum computing

Yuchen Wang¹, Zixuan Hu¹, Barry C. Sanders*², and Sabre Kais^{†1}

¹Department of Chemistry, Department of Physics and Purdue Quantum Science and Engineering Institute, Purdue University, West Lafayette, Indiana 47907, USA

²Institute for Quantum Science and Technology, University of Calgary, Alberta T2N 1N4, Canada

June 12, 2022

Abstract

Qudit is a multi-level computational unit alternative to the conventional 2-level qubit. Compared to qubit, qudit provides a larger state space to store and process information, and thus can provide reduction of the circuit complexity, simplification of the experimental setup and enhancement of the algorithm efficiency. This review provides an overview of qudit-based quantum computing covering a variety of topics ranging from circuit building, algorithm design, to experimental methods. We first discuss the qudit gate universality and a variety of qudit gates including the $\pi/8$ gate, the SWAP gate, and the multi-level controlled-gate. We then present the qudit version of several representative quantum algorithms including the Deutsch-Jozsa algorithm, the quantum Fourier transform, and the phase estimation algorithm. Finally we discuss various physical realizations for qudit computation such as the photonic platform, ion trap, and nuclear magnetic resonance.

1 Introduction to qudits

Qudit technology, with a qudit being a quantum version of d -ary digits for $d > 2$ [1], is emerging as an alternative to qubits for quantum computation and quantum information science. Due to its multi-level nature, qudit provides a larger state space to store and process information and the ability to do multiple control operations simultaneously [2]. These features play an important role in the reduction of the circuit complexity, the simplification of the experimental setup and the enhancement of the algorithm efficiency [3, 4, 5, 2]. The advantage

*sandersb@ucalgary.ca

†kais@purdue.edu

of the qudit not only applies to the circuit model for quantum computers but also applies to adiabatic quantum computing devices [6, 7], topological quantum systems [8, 9, 10] and more. The qudit-based quantum computing system can be implemented on various physical platforms such as photonic systems [2, 11], continuous spin systems [12, 13], ion trap [14], nuclear magnetic resonance [15, 16] and molecular magnets [17].

Although the qudit systems advantages in various applications and potentials for future development are substantial, this system receives less attention than the conventional qubit-based quantum computing, and a comprehensive review of the qudit-based models and technologies is needed. This review article provides an overview of qudit-based quantum computing covering a variety of topics ranging from circuit building [18, 19, 20, 21, 22], algorithm design [16, 23, 24, 13, 25, 26, 27], to experimental methods [2, 11, 12, 13, 14, 15, 16, 17]. In this article, high-dimensional generalizations of many widely used quantum gates are presented and the universality of the qudit gates is shown. Qudit versions of three major classes of quantum algorithms—algorithms for the oracles decision problems (e.g., the Deutsch-Jozsa algorithm [23]), algorithms for the hidden non-abelian subgroup problems (e.g. the phase-estimation algorithms (PEAs) [25]) and the quantum search algorithm (e.g. the Grover's algorithm [27])—are discussed and the comparison of the qudit designs versus the qubit designs is analyzed. Finally, we introduce various physical platforms that can implement qudit computation and compare their performances with their qubit counterparts.

Our article is organized as follows. Definitions and properties of a qudit and related qudit gates are given in §2. The generalization of the universal gate set to qudit systems and several proposed sets are provided in §2.1. Then §2.2 lists various examples of qudit gates and discusses the difference and possible improvement of these gates over their qubit counterparts. A discussion of the gate efficiency of synthesizing an arbitrary unitary U using geometric method is given in §2.3. The next section, §3, provides an introduction to qudit algorithms: a single-qudit algorithm that finds the parity of a permutation in §3.1.1, the Deutsch-Jozsa algorithm in §3.1.2, the Bernstein-Vazirani algorithm in §3.1.3, the quantum Fourier transform in §3.2.1, the PEA in §3.2.2 and the quantum search algorithm in §3.3. In §4, we provide various realizations of the qudit algorithms on physical platforms and discuss their applications. We discuss possible improvements in computational speed-up, resource saving and implementations on physical platforms. A qudit with a larger state space than a qubit can utilize the full potential of physical systems such as photon in §4.1, ion trap in §4.2, nuclear magnetic resonance in §4.3 and molecular magnet in §4.4. Finally, we give a summary of the qudit systems and provide our perspective for the future developments and applications of the qudit in §5.

2 Quantum gates for qudits

A *qudit* is a quantum version of d -ary digits whose state can be described by a vector in the d dimensional Hilbert space \mathcal{H}_d [1]. The space is spanned by a set of orthonormal basis vectors $\{|0\rangle, |1\rangle, |2\rangle, \dots, |d-1\rangle\}$. The state of a qudit has the general form

$$|\alpha\rangle = \alpha_0 |0\rangle + \alpha_1 |1\rangle + \alpha_2 |2\rangle + \dots + \alpha_{d-1} |d-1\rangle = \begin{pmatrix} \alpha_0 \\ \alpha_1 \\ \alpha_2 \\ \vdots \\ \alpha_{d-1} \end{pmatrix} \in \mathbb{C}^d \quad (1)$$

where $|\alpha_0|^2 + |\alpha_1|^2 + |\alpha_2|^2 + \dots + |\alpha_{d-1}|^2 = 1$. Qudit can replace qubit as the basic computational element for quantum algorithms. The state of a qudit is transformed by qudit gates.

This section gives a review of various qudit gates and their applications. §2.1 provides criteria for the qudit universality and introduces several fundamental qudit gate sets. §2.2 presents examples of qudit gates and illustrates their advantages compared to qubit gates. In the last section, §2.3, a quantitative discussion of the circuit efficiency is included to give a boundary of the number of elementary gates needed for decomposing an arbitrary unitary matrix.

2.1 Criteria for universal qudit gates

This subsection describes the universal gates for qudit-based quantum computing and information processing. We elaborate on the criteria for universality in §2.1.1 and give examples in §2.1.2.

2.1.1 Universality

In quantum simulation and computation, a set of matrices $U_k \in U(d^n)$ is called the universal quantum gate set if the product of its elements can be used to approximate any arbitrary unitary transformation U of the Hilbert space $\mathcal{H}_d^{\otimes n}$ with acceptable error measured in some appropriate norm [28]. This idea of *universality* not only applies to the qubit systems [29], but can also be extended to the qudit logic [30, 19, 31, 32, 33, 34]. Several discussions of standards and proposals for a universal qudit gate set exist. Vlasov shows that the combination of two noncommuting single qudit gates and a two-qudit gate are enough to simulate any unitary $U \in U(d^n)$ with arbitrary precision [28]. Qudit gates can themselves be reduced to, and thus simulated by, sequences of qudit gates of lower-dimensional qudit gates [35, 36] Brylinski and Brylinski prove a set of sufficient and necessary conditions for exact qudit universality which needs some random single qudit gates complemented by one two-qudit gate that has entangled qudits [1]. Exact universality implies that any unitary gate and any quantum process can be simulated with zero error. Neither of these methods is

constructive and includes a method for physical implementation. A physically workable procedure is given by Muthukrishnan and Stroud using single- and two-qudit gates to decompose an arbitrary unitary gate that operates on N qudits [37]. They use the spectral decomposition of unitary transformations and involve a gate library with a group of continuous parameter gates. Brennen et al. identify criteria for exact quantum computation in qudit that relies on the QR decomposition of unitary transformations [38]. They generate a library of gates with a fixed set of single qudit operations and "one controlled phase" gate with single parameter as the components of the universal set. Implementing the concept of a coupling graph, they proved that by connecting the nodes (equivalently logical basis states) they can show the possibility of universal computation.

2.1.2 Examples of universal gate sets

An explicit and physically realizable universal set comprising one-qudit general rotation gates and two-qudit controlled extensions of rotation gates is explained in this section [3]. We first define

$$U_d(\boldsymbol{\alpha}) : \sum_{l=0}^{d-1} \alpha_l |l\rangle \mapsto |d-1\rangle, \boldsymbol{\alpha} := (\alpha_0, \alpha_1, \dots, \alpha_{d-1}). \quad (2)$$

as a transformation in the d -dimensional space that maps any given qudit state to $|d-1\rangle$. Complex parameters of U_d may not be unique and have been addressed with probabilistic quantum search algorithm [37]. Here in this scheme, U_d can be deterministically decomposed into $d-1$ unitary transformations such that

$$U_d = X_d^{(d-1)}(a_{d-1}, b_{d-1}) \cdots X_d^{(1)}(a_1, b_1), \quad a_l := \alpha_l, \quad b_l := \sqrt{\sum_{i=0}^{l-1} \alpha_i^2} \quad (3)$$

with

$$X_d^{(l)}(x, y) = \begin{pmatrix} \mathbb{1}_{l-1} & & & \\ & \frac{x}{\sqrt{|x|^2+|y|^2}} & \frac{-y}{\sqrt{|x|^2+|y|^2}} & \\ & \frac{y^*}{\sqrt{|x|^2+|y|^2}} & \frac{x^*}{\sqrt{|x|^2+|y|^2}} & \\ & & & \mathbb{1}_{d-l-1} \end{pmatrix}. \quad (4)$$

The d -dimensional phase gate is

$$Z_d(\theta) := \sum_{l=0}^{d-1} e^{i(1-\text{sgn}(d-1-l))\theta} |l\rangle \langle l|, \quad (5)$$

which changes $|d-1\rangle$ by a phase θ and ignores the other states, and sgn represents the sign function.

Each primitive gate (such as $X_d^{(l)}$ or Z_d) has two free complex parameters to be controlled (x, y in the $X_d^{(l)}$ gate and θ in the Z_d gate). Let R_d represents

either $X_d^{(l)}$ or Z_d , then the controlled-qudit gate is

$$C_2[R_d] := \begin{pmatrix} \mathbb{1}_{d^2-d} & \\ & R_d \end{pmatrix}, \quad (6)$$

which is a $d^2 \times d^2$ matrix that acts on two qudits. R_d acts on d substates $|d-1\rangle|0\rangle, \dots, |d-1\rangle|d-1\rangle$, and the identity operation $\mathbb{1}_{d^2-d}$ acts on the remaining substates.

Now we work on an $N = d^n$ dimensional unitary gate $U \in SU(d^n)$ operating on the n -qudit state. The sufficiency of the gates $X_d^{(l)}, Z_d$ and $C_2[R_d]$ to construct an arbitrary unitary transformation of $SU(d^n)$ is proved in three steps. The first step is the eigen-decomposition of U . By the representation theory, the unitary matrix U with N eigenvalues $\{\lambda_s\}$ and eigenstates $|E_s\rangle$ can be rewritten as

$$U = \sum_{j=1}^N e^{i\lambda_j} |E_j\rangle \langle E_j| = \prod_{j=1}^N \Upsilon_j \quad (7)$$

with eigenoperators

$$\Upsilon_j = \sum_{s=1}^N e^{i(1-|\text{sgn}(j-s)|)\lambda_s} |E_s\rangle \langle E_s|. \quad (8)$$

Then the eigenoperators can be synthesized with two basic transformations as [37]

$$\Upsilon_j = U_{j,N}^{-1} Z_{j,N} U_{j,N}. \quad (9)$$

Here $U_{j,N}$ and $Z_{j,N}$ are the N -dimensional analogues of U_d and Z_d such that $U_{j,N}$ is applied to the j th eigenstate to produce $|N-1\rangle$ and $Z_{j,N}$ modifies the phase of $|N-1\rangle$ by the j th eigenphase λ_j , while ignoring all the other computation states. According to Eq. (3), $U_{j,N}$ can be decomposed with primitive gates $X_{j,N}^{(l)}(x, y)$. Thus, $X_{j,N}(x, y)$ and $Z_{j,N}$ are sufficient to decompose U .

The second step is decomposing $U_{j,N}$ and $Z_{j,N}$. In other words, $U_{j,N}$ and $Z_{j,N}$ need to be decomposed in terms of multi-qudit-controlled gates. For convenience denote $C_m[R_d]$ as

$$C_m[R_d] = \begin{pmatrix} \mathbb{1}_{d^m-d} & \\ & R_d \end{pmatrix}, \quad (10)$$

which acts on the d^m -dimensional computational basis of m -qudit space. It is proved in the appendix of Ref. [3] that each $U_{j,N}$ can be decomposed into some combinations of $C_m[R_d]$ and $C_m[P_d(p, q)]$ where $P_d(p, q)$ is the permutation of $|p\rangle$ and $|q\rangle$ state. The third step is using the two-qudit gates $C_2[R_d]$ and $C_2[P_d(p, q)]$ to complete the decomposition of $C_m[R_d]$. Fig. 1 shows a possible decomposition for $d > 2$. There are $r = \lceil (m-2)/(d-2) \rceil$ auxiliary qudits in the circuits ($\lceil x \rceil$ denotes the smallest integer greater than x). The last box contains $R_d = Z_d$ or $X_d^{(l)}$. $C_m[R_d]$ is implemented with these gates combined. All of the three steps together prove that the qudit gates set

$$\Gamma_d := \{X_d^{(l)}, Z_d, C_2[R_d]\} \quad (11)$$

is universal for the quantum computation using qudit systems.

The total number of primitive operations in this decomposition method is

$$L \leq 2N \times 3d^{n-1} \times n \times (d-2) + N \times n \leq 6nd^{2n} + nd^n. \quad (12)$$

One advantage of this qudit model (compared to the qubit model) is a reduction of the number of qudits required to span the state space. To explain this, we need at least $n_1 = \log_2 N$ qubits to represent an N -dimensional system in qubits while in qudits we need $n_2 = \log_d N$ qudits. The qudit system has a reduction factor $k = n_1/n_2 = \log_2 d$. The other advantage is these primitive qudit gates can be easily implemented with fewer free parameters [3].

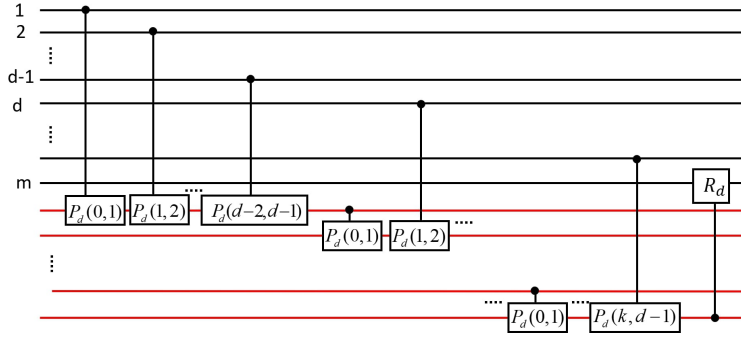


Figure 1: The schematic circuit of $C_m[R_d]$ with $C_2[R_d]$ and $C_2[P_d(p, q)]$. The horizontal lines represent qudits. The auxiliary qudits initialized to $|0\rangle$ is denoted by the red lines and the black lines denoting m controlling qudits. The two-qudit controlled gates is shown as the vertical lines. $P_d(p, q)$ is the permutation of $|p\rangle$ and $|q\rangle$ state, and R_d is either $X_d^{(l)}$ or Z_d .

For qudit quantum computing, depending on the implementation platform, other universal quantum gate sets can be considered. For example, in a recent proposal for topological quantum computing with metaplectic anyons, Cui and Wang prove a universal gates set for qutrit and *qupit* systems, for a qupit being a qudit with p dimensions and p is an odd prime number larger than 3 [8]. The proposed universal set is a qudit analogy of the qubit universal set and it consists several generalized qudit gates from the universal qubit set.

The generalized Hadamard gate for qudits H_d is

$$H_d |j\rangle = \frac{1}{\sqrt{d}} \sum_{i=0}^{d-1} \omega_d^{ij} |i\rangle, j+1 \in [d] := \{1, \dots, d\}, \quad (13)$$

where

$$\omega := e^{2\pi i/d}. \quad (14)$$

The SUM_d gate serves as a natural generalization of the CNOT gate

$$\text{SUM}_d |i, j\rangle = |i, i+j(\text{mod } d)\rangle, i+1, j+1 \in [d]. \quad (15)$$

The Pauli σ_z , with the $\pi/8$ gate as its 4th root, can be generalized to $Q[i]$ gates for qudits,

$$Q[i]_d |j\rangle = \omega_d^{\delta_{ij}} |j\rangle, \quad (16)$$

with ω defined by Eq. (14) and the related $P[i]$ gates are

$$P[i]_d |j\rangle = (-\omega_d^2)^{\delta_{ij}} |j\rangle, \quad i+1, j+1 \in [d]. \quad (17)$$

In general $Q[i]_p$ is always a power of $P[i]_p$ if p is an odd prime .

The proposed gate set for the qutrit system is the sum gate SUM_3 , the Hadamard gate H_3 and any gate from the set $\{P[0]_3, P[1]_3, P[2]_3\}$. As an analogue of the standard universal set for qubit $\{\text{CNOT}, H, T = \pi/8\text{-gate}\}$, the qutrit set generate the qutrit Clifford group whereas the qubit set generate the qubit Clifford group (the definition of the Clifford group can be found in §2.2.1). Whereas the rigorous proof can be found in Ref. [8], the proving process follows the idea introduced in Ref. [1] that the gate SUM_3 is imprimitive, and the Hadamard H_3 and any gate from $\{P[0]_3, P[1]_3, P[2]_3\}$ generates a dense subgroup of $SU(3)$. Similarly, the proposed gate set for the qupit system is the sum gate SUM_p , the Hadamard gate H_p and the gates $Q[i]_p$ for $i \in [p-1]$. The proof is analogous to that of the qutrit set. The Hadamard H_p and the $Q[i]_p$ gates are combined to form a dense subgroup of $SU(p)$ and SUM_p is shown to be imprimitive. Implementing Theorem 1.3 in Ref. [1], the set is a universal gate set. These universal gate sets for the qudit systems, with fewer numbers of gates in each set compare to that in the previous examples, have the potential to perform qudit quantum algorithms on the topological quantum computer.

2.2 Examples of qudit gates

In this section we introduce the qudit versions of many important quantum gates and discuss some of the gates' advantages compared to their qubit counterparts. The gates discussed are the qudit versions of the $\pi/8$ gate in §2.2.1, the SWAP gate in §2.2.2 and the multi-level controlled gate in §2.2.4. in §2.2.3, we also introduce how to simplify the qubit Toffoli gate by replacing one of the qubit to qudit. This gives ideas about improving the qubit circuits and gates by introducing qudits to the system.

2.2.1 Qudit versions $\pi/8$ gate

The qubit $\pi/8$ gate T has an important role in quantum computing and information processing. This gate has a wide range of applications because it is closely related to the Clifford group but does not belong to the group. From the Gottesman-Knill theorem [39] it is shown that the Clifford gates and Pauli measurements only do not guarantee universal quantum computation(UQC). The $\pi/8$ gate, which is non-Clifford and from the third level of the Clifford hierarchy, is the essential gate to obtaining UQC [40]. This gate can be generalized to a d dimensional qudit system, where, throughout the process, d is assumed to be a prime number greater than 2 [18].

To define the Clifford group for a d -dimensional qudit space, we first define the Pauli Z gate and Pauli X gate. The Pauli Z gate and Pauli X gate are generalized to d dimension in the matrix forms [41, 42, 12, 43]

$${}^dX = \begin{pmatrix} 0 & 0 & \cdots & 0 & 1 \\ 1 & 0 & \cdots & 0 & 0 \\ 0 & 1 & \cdots & 0 & 0 \\ \vdots & \vdots & \ddots & \vdots & \vdots \\ 0 & 0 & \cdots & 1 & 0 \end{pmatrix}, \quad {}^dZ = \begin{pmatrix} 1 & 0 & 0 & \cdots & 0 \\ 0 & \omega & 0 & \cdots & 0 \\ 0 & 0 & \omega^2 & \cdots & 0 \\ \vdots & \vdots & \vdots & \ddots & \vdots \\ 0 & 0 & 0 & \cdots & \omega^{d-1} \end{pmatrix} \quad (18)$$

for ω the d^{th} root of unity (14). The function of the Z gate is adding different phase factors to each basis states and that of the X gate is shifting the basis state to the next following state. Using basis states the two gates are

$$Z|j\rangle := \omega^j|j\rangle \quad X|j\rangle := |j+1\rangle, \quad j \in \{0, 1, 2, \dots, d-1\}. \quad (19)$$

In general, we define the displacement operators as products of the Pauli operators,

$$D_{(x|z)} = \tau^{xz} X_d^x Z_d^z, \quad \tau := e^{(d+1)\pi i/d} = \omega^{2^{-1}}. \quad (20)$$

This leads to the definition of the Weyl-Heisenberg group (or the generalized Pauli group) for a single qudit as [41, 42, 12, 43]

$$\mathcal{G} = \{\tau^c D_{\vec{\chi}} | \vec{\chi} \in \mathbb{Z}_d^2, c \in \mathbb{Z}_d\} \quad (\mathbb{Z}_d = \{0, 1, \dots, d-1\}), \quad (21)$$

where $\vec{\chi}$ is a two-vector with elements from \mathbb{Z}_d . With these preliminary concepts defined in Eqs. (18) through (21), we now define the Clifford group as the following: the set of the operators that maps the Weyl-Heisenberg group onto itself under conjugation is called the *Clifford group* [43, 44],

$$\mathcal{C} = \{C \in U(d) | C\mathcal{G}C^\dagger = \mathcal{G}\}. \quad (22)$$

A recursively defined set of gates, the so-called Clifford hierarchy, was introduced by Gottesman and Chuang as

$$\mathcal{C}_{k+1} = \{U|U\mathcal{C}_1U^\dagger \subseteq \mathcal{C}_k\}, \quad (23)$$

for \mathcal{C}_1 the Pauli group [45]. The sets $\mathcal{C}_{k \geq 3}$ do not form groups, although the diagonal subsets of \mathcal{C}_3 , which is our focus here, do form a group.

The following derivations follow those in Ref. [18]. The explicit formula for building a Clifford unitary gate with

$$F = \begin{pmatrix} \alpha & \beta \\ \gamma & \delta \end{pmatrix} \in \text{SL}(2, \mathbb{Z}_d), \quad \vec{\chi} = \begin{pmatrix} x \\ z \end{pmatrix} \in \mathbb{Z}_d^2 \quad (24)$$

is

$$C_{(F|\vec{\chi})} = D_{(x|z)} V_F, \quad (25)$$

$$V_F = \begin{cases} \frac{1}{\sqrt{d}} \sum_{j,k=0}^{d-1} \tau^{\beta^{-1}(\alpha k^2 - 2jk + \delta j^2)} |j\rangle \langle k|, & \beta \neq 0 \\ \sum_{k=0}^{d-1} \tau^{\alpha \gamma k^2} |\alpha k\rangle \langle k|, & \beta = 0. \end{cases} \quad (26)$$

The special case $\beta = 0$ is particularly relevant to the later derivation, and

$$\begin{aligned} \det \left(\sum_{k=0}^{d-1} \tau^{\alpha \gamma k^2} |k\rangle \langle k| \right) &= \tau^{\frac{\alpha \gamma}{8} (2d-1)(d-1)d}, \\ &= \begin{cases} \tau^{2\alpha \gamma}, & d = 3, \\ 1, & \forall d > 3, \end{cases} \end{aligned} \quad (27)$$

can be shown. In the $d = 3$ case, we use

$$C \left(\begin{array}{c|c} \begin{bmatrix} 1 & 0 \\ \gamma & 1 \end{bmatrix} & \begin{bmatrix} x \\ z \end{bmatrix} \end{array} \right) \in SU(p) \quad \forall p > 3 \quad (28)$$

and

$$\det \left(C \left(\begin{array}{c|c} \begin{bmatrix} 1 & 0 \\ \gamma & 1 \end{bmatrix} & \begin{bmatrix} x \\ z \end{bmatrix} \end{array} \right) \right) = \tau^{2\gamma} \text{ for } p = 3. \quad (29)$$

With all the mathematical definitions at hand, we are ready to give an explicit form of the qudit $\pi/8$ gate. We choose the qudit gate U_v to be diagonal in the computational basis and claim that, for $d > 3$, U_v has the form

$$U_v = U(v_0, v_1, \dots) = \sum_{k=0}^{d-1} \omega^{v_k} |k\rangle \langle k| \quad (v_k \in \mathbb{Z}_d). \quad (30)$$

A straightforward application of Eqs. (20) and (30) yields

$$U_v D_{(x|z)} U_v^\dagger = D_{(x|z)} \sum_k \omega^{v_{k+1} - v_k} |k\rangle \langle k|. \quad (31)$$

As U_v is to be a member of \mathcal{C}_3 , the right hand side of Eq. (31) must be a Clifford gate. We ignore the trivial case $U_v D_{(0|z)} U_v^\dagger = D_{(0|z)}$ and focus on the case $U_v D_{(1|0)} U_v^\dagger$ in order to derive an explicit expression for U_v .

We define $\gamma', z', \epsilon' \in \mathbb{Z}_d$ such that

$$U_v D_{(1|0)} U_v^\dagger = \omega^{\epsilon'} C \left(\begin{array}{c|c} \begin{bmatrix} 1 & 0 \\ \gamma' & 1 \end{bmatrix} & \begin{bmatrix} 1 \\ z' \end{bmatrix} \end{array} \right) \quad (32)$$

From Eqs. (26) and (31) we see that the right-hand side of Eq. (32) is the most general form, and we note that $U \in SU(d)$ implies $\omega^{\gamma'} U \in SU(d)$. We rewrite the left-hand side of Eq. (32) using Eq. (31) and right-hand side using Eq. (26) and obtain

$$D_{(1|0)} \sum_k \omega^{v_{k+1} - v_k} |k\rangle \langle k| = \omega^{\epsilon'} D_{(1|z')} \sum_{k=0}^{d-1} \tau^{\gamma' k^2} |k\rangle \langle k|. \quad (33)$$

After cancelling common factors of $D_{(1|0)}$, an identity between two diagonal matrices remains such that

$$\omega^{v_{k+1}-v_k} = \omega^{\epsilon'} \tau^{z'} \omega^{kz'} \tau^{\gamma' k^2} \quad (\forall k \in \mathbb{Z}_d), \quad (34)$$

or, equivalently, using Eq. (20),

$$v_{k+1} - v_k = \epsilon' + 2^{-1}z' + kz' + 2^{-1}\gamma'k^2. \quad (35)$$

From here, we derive the recursive relation

$$v_{k+1} = v_k + k(2^{-1}\gamma'k + z') + 2^{-1}z' + \epsilon'. \quad (36)$$

We solve for the v_k with a boundary condition $v_0 = 0$,

$$v_k = \frac{1}{12}k\{\gamma' + k[6z' + (2k-3)\gamma']\} + k\epsilon', \quad (37)$$

where all factors are evaluated modulo d . For example, with $d = 5$, the fifth root of unity (14) is $\omega = e^{2\pi i/5}$ and choosing $z' = 1$, $\gamma' = 4$ and $\epsilon' = 0$, we obtain

$$v = (v_0, v_1, v_2, v_3, v_4) = (0, 3, 4, 2, 1) \quad (38)$$

so that

$$U_v = \begin{pmatrix} \omega^0 & 0 & 0 & 0 & 0 \\ 0 & \omega^{-2} & 0 & 0 & 0 \\ 0 & 0 & \omega^{-1} & 0 & 0 \\ 0 & 0 & 0 & \omega^2 & 0 \\ 0 & 0 & 0 & 0 & \omega^1 \end{pmatrix} \quad (39)$$

The diagonal elements of U_v are powers of ω that sum to zero modulo d and, consequently, $\det(U_v) = 1$.

For the $d = 3$ case, because of Eq. (27) extra work is needed for solving a matrix equation similar to Eq. (32). We first introduce a global phase factor $e^{i\phi}$ such that

$$\det \left(e^{i\phi} \sum_{k=0}^{d-1} \tau^{\gamma k^2} |k\rangle \langle k| \right) = 1 \implies \phi = 4\pi\gamma/9. \quad (40)$$

The ninth root of unity (14) is $\omega = e^{2\pi i/9}$ and, from Eq. (29) we derive that

$$\det \left(\omega^{2\gamma'} C \left(\begin{bmatrix} 1 & 0 \\ \gamma' & 1 \end{bmatrix} \middle| \begin{bmatrix} 1 \\ z' \end{bmatrix} \right) \right) = 1. \quad (41)$$

The qutrit version of $U_{\pi/8}$ has a more general form than in Eq. (30); i.e.

$$U_v = U(v_0, v_1, \dots) = \sum_{k=0}^2 \omega^{v_k} |k\rangle \langle k|, \quad v_k \in \mathbb{Z}_9. \quad (42)$$

Then the general solution is

$$v = (0, 6z' + 2\gamma' + 3\epsilon', 6z' + \gamma' + 6\epsilon') \pmod{9}. \quad (43)$$

For example, choosing $z' = 1, \gamma' = 2$ and $\epsilon' = 0$,

$$U_v = \begin{pmatrix} \omega^0 & 0 & 0 \\ 0 & \omega^1 & 0 \\ 0 & 0 & \omega^{-1} \end{pmatrix}. \quad (44)$$

The $\pi/8$ gate, with its close relation to the Clifford group has many applications and utilities in teleportation-based UQC [45], transversal implementation [46, 47], learning an unknown gate [48], or securing assisted quantum computation [49]. The generalized qudit version of the $\pi/8$ gate, U_v , is shown to be identical to the maximally robust qudit gates for qudit fault-tolerant UQC discussed in reference [50].

This gate also plays an important role in the magic-state distillation (MSD) protocols for general qudit systems, which was first established for qutrits [51] and then extended to all prime-dimensional qudits [52].

2.2.2 Qudit SWAP gate

A SWAP gate is used to exchange the states of two qudit such that:

$$\text{SWAP}|\phi\rangle|\psi\rangle = |\psi\rangle|\phi\rangle \quad (45)$$

Various methods to achieve the SWAP gate use different variants of qudit controlled gates [53, 54, 55, 56, 57, 58, 59] as shown in Fig.2. The most used component of the SWAP gate is a controlled-shift gate CX_d that perform the following operation:

$$CX_d|x\rangle|y\rangle = |x\rangle|x+y\rangle \quad (46)$$

with a modulo d addition. Its inverse operation is

$$CX_d^\dagger|x\rangle|y\rangle = |x\rangle|y-x\rangle \quad (47)$$

In some approaches, the operation X_d is required to complete the circuits, where

$$X_d|x\rangle = |d-x\rangle = |-x\rangle, \quad (48)$$

which outputs the modulo d complement of the input. These circuits are more complex and less intuitive than the qubit SWAP gate [56] because they are not Hermitian, i.e., $CX_d \neq CX_d^\dagger$.

One way to create a Hermitian version of the qudit CNOT uses the GXOR gate

$$GXOR|x\rangle|y\rangle = |x\rangle|x-y\rangle. \quad (49)$$

However, this SWAP gate needs to be corrected with an X_d [59] as shown in Fig. 3. A partial SWAP gate S_p [19] works on a hybrid system where $|i\rangle$ is a qudit of dimension d_c and $|j\rangle$ is a qudit of dimension d_t

$$S_p |i\rangle \otimes |j\rangle = \begin{cases} |j\rangle \otimes |i\rangle & \text{for } i, j \in \mathbb{Z}_{d_p} \\ |i\rangle \otimes |j\rangle & \text{otherwise} \end{cases} \quad (50)$$

where $d_p \leq d_{\min} = \min(d_c, d_t)$

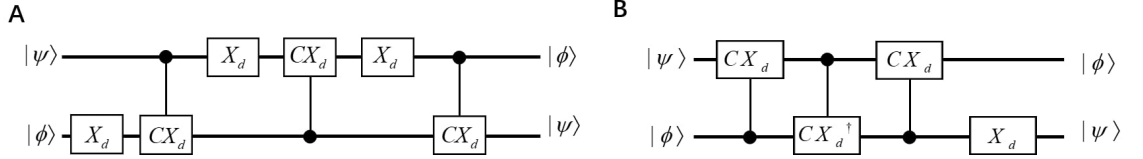


Figure 2: **(A)** is the qudit SWAP circuit using CX_d and X_d gates[56, 57]. **(B)** is the qudit SWAP circuits with the CX_d , the CX_d^\dagger and the X_d gates

In the rest of this section, we present a Hermitian generalization of the qudit CNOT gate with a symmetry configuration and a qudit SWAP circuit with a single type of qudit gate as shown in Fig. 4 **A** [20]. Compared with all the previously proposed SWAP gate for qudit, this method is easier to implement since there is only one type of gate $C\tilde{X}$ needed. To begin with, we define a gate $C\tilde{X}$ acting on d -level qudits $|x\rangle$ and $|y\rangle$ such that

$$C\tilde{X} |x\rangle |y\rangle = |x\rangle |-x - y\rangle, \quad (51)$$

where $|-x - y\rangle$ represents a state $|i = -x - y\rangle$ in the range $i \in \{0, \dots, d-1\} \bmod d$. Notice that, for $d = 2$, the $C\tilde{X}$ gate is equivalent to the CNOT gate. The SWAP gate for qudit can be built using three $C\tilde{X}$ gates.

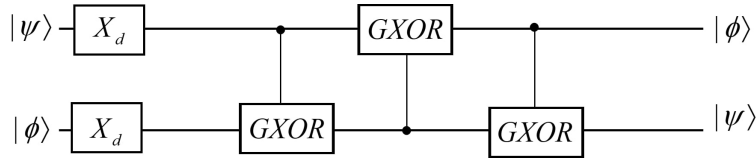


Figure 3: Qudit SWAP circuits with the $GXOR$ and the X_d gates.[58, 59]

$C\tilde{X}$ is generated with three steps: a qudit generalization of the CZ gate as CZ_d sandwiched by two quantum Fourier transform operations(QFT). The circuit illustration for the sequence of these gate is shown in Fig. 4 **B**. The QFT transforms the $|x\rangle$ into a uniform superposition

$$QFT |x\rangle = \frac{1}{\sqrt{d}} \sum_{k=0}^{d-1} e^{i2\pi xk/d} |k\rangle. \quad (52)$$

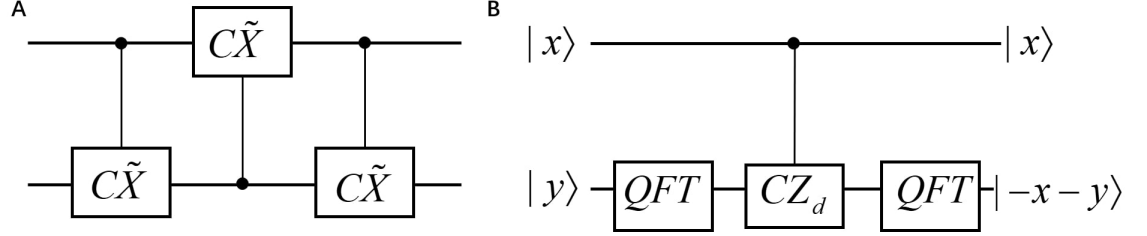


Figure 4: **(A)** is the qudit SWAP gate with the $C\tilde{X}$ gate. **(B)** is the decomposing $C\tilde{X}$ gate. The QFT represents the quantum Fourier transform while CZ_d is the selective phase shift gate.

The CZ_d gate adds a phase to the target qudit depending on the state of the control qudit. Its effect on the input qudits is

$$CZ_d |x\rangle |y\rangle = e^{i2\pi xy/d} |x\rangle |y\rangle. \quad (53)$$

The inverse QFT undoes the Fourier transform process and the inverse of CZ_d is

$$CZ_d^\dagger |x\rangle |y\rangle = e^{-i2\pi xy/d} |x\rangle |y\rangle. \quad (54)$$

The full evolution of the $C\tilde{X}$ is

$$|x\rangle |y\rangle \xrightarrow{QFT_2} \frac{1}{\sqrt{d}} \sum_{k=0}^{d-1} e^{i\frac{2\pi ky}{d}} |x\rangle |k\rangle \quad (55)$$

$$\xrightarrow{CZ_d} \frac{1}{\sqrt{d}} \sum_{k=0}^{d-1} e^{i\frac{2\pi ky}{d}} e^{i\frac{2\pi xk}{d}} |x\rangle |k\rangle = \frac{1}{\sqrt{d}} \sum_{k=0}^{d-1} e^{i\frac{2\pi k(x+y)}{d}} |x\rangle |k\rangle \quad (56)$$

$$\xrightarrow{QFT_2} \frac{1}{d} \sum_{l=0}^{d-1} \sum_{k=0}^{d-1} e^{i\frac{2\pi k(x+y)}{d}} e^{i\frac{2\pi kl}{d}} |x\rangle |l\rangle = |x\rangle | -x - y \rangle. \quad (57)$$

It is easy to show that $C\tilde{X}$ is its own inverse and then $C\tilde{X} = C\tilde{X}^\dagger$. For the proposed SWAP gate, both the QFT and CZ_d operations are realizable on a multilevel quantum systems. For example, there are implementations of them for multilevel atoms [37, 60]. The resulting SWAP gate provides a way to connect systems limited to the nearest-neighbour interactions. This gate provides a useful tool in the design and analysis of complex qudit circuits.

2.2.3 Simplified qubit Toffoli gate with a qudit

The Toffoli gate is well known for its application to universal reversible classical computation. In the field of quantum computing, the Toffoli gate plays a central role in quantum error correction [61], fault tolerance [62] and offers a simple universal quantum gate set combined with one qubit Hadamard gates [63]. The

simplest known qubit Toffoli gate, shown in Fig. 5, requires at least 5 two-qubit gates [64]. However, if the target qubit has a third level, i.e., a qutrit, the whole circuit can be achieved with three two-qubit gates [21].

A new qutrit gate X_a is introduced to the circuit that does the following: $X_a|0\rangle = |2\rangle$ and $X_a|2\rangle = |0\rangle$ with $X_a|1\rangle = |1\rangle$. The simplified circuit is shown in Fig. 6. The two controlled gates are the CNOT gate and a control- Z gate, which is achieved with a CNOT gate between two Hadamard gates. The Hadamard gate here operating on a qutrit is generalized from the normal Hadamard gate operating on a qubit—it only works with the $|0\rangle$ and $|1\rangle$, such that $H|0\rangle = 1/\sqrt{2}[|0\rangle + |1\rangle]$, $H|1\rangle = 1/\sqrt{2}[|0\rangle - |1\rangle]$ and $H|2\rangle = |2\rangle$. Comparing the circuit in Fig. 6 to that in Fig. 5, it is clear that the total number of gates is significantly reduced.

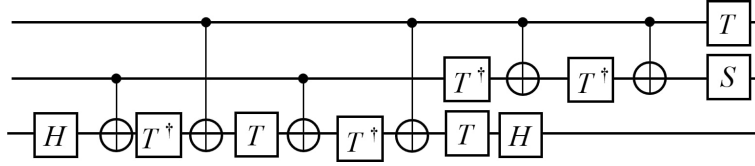


Figure 5: Decomposing qubit Toffoli gate with the universal qubit gates. H is the Hadamard gate, T is the $\pi/8$ gate and S is the phase gate.

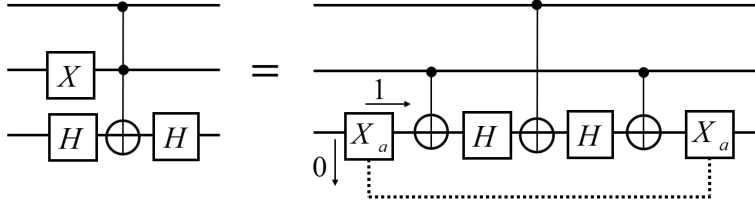


Figure 6: The Simplified Toffoli gate. The first two lines represent two control qubits and the third line represents a target qutrit that has three accessible levels. The initial and final quantum states of the quantum information carrier are encoded in the $|0\rangle$ and $|1\rangle$. The H is the generalized Hadamard gate such that $H|0\rangle = 1/\sqrt{2}[|0\rangle + |1\rangle]$, $H|1\rangle = 1/\sqrt{2}[|0\rangle - |1\rangle]$ and $H|2\rangle = |2\rangle$. X_a gate is a qutrit gate such that $X_a|0\rangle = |2\rangle$ and $X_a|2\rangle = |0\rangle$ with $X_a|1\rangle = |1\rangle$. With the control being qubit, the target being qutrit, the two qutrit gate in this case is a hybrid gate.

This method can be generalized to n -qubit-controlled Toffoli gates by utilizing a single $(n+1)$ -level target carrier and using only $2n-1$ two-qubit gates [21]. In other words, the target carrier needs an extra level for each extra control qubit. Compare to the best known realization previously that requires $12n-11$ two-qubit gates [64], this method offers a significant resource reduction. Fur-

thermore, these schemes can be extended to more general quantum circuits such as the multi-qudit-controlled-unitary gate $C^n U$.

The previous method turns the target qubit into a qudit; another method simplifies the Toffoli gate by using only qudits and treating the first two levels of the qudit as qubit levels and other levels as auxiliary levels. The reduction in the complexity of Toffoli gate is accomplished by utilizing the topological relations between the dimensionality of the qudits, where higher qudit levels serve as the ancillas [22].

Suppose we have a system of n qudits denoted as Q_i , $i \in \{1, \dots, n\}$ and each qudit has dimension $d_i \geq 2$. Qudits are initialized into pure or mix states on the first two levels, i.e., the qubit states, and zero population for the other levels, i.e., the auxiliary states. This scheme assumes the ability to perform single-qubit operations. We can apply the desirable unitary operation on the qubit states and leave the auxiliary states unchanged. We also assume that we have the ability to manipulate the auxiliary levels by a generalized inverting gate X_m

$$X_m |0\rangle = |m\rangle, X_m |m\rangle = |0\rangle, X_m |y\rangle = |y\rangle, \text{ for } y \neq m, 0. \quad (58)$$

At the same time, the two-qubit CZ gates are applied according to certain topological connections between qudits. We introduce a set E of ordered pairs (i, j) , such that $i, j \in \{1, \dots, n\}$, $i < j$ to obtain this topology and the CZ gate is defined as

$$CZ |11\rangle_{Q_i, Q_j} = -|11\rangle_{Q_i, Q_j}, CZ |xy\rangle_{Q_i, Q_j} = |xy\rangle_{Q_i, Q_j} \text{ for } xy \neq 1, \quad (59)$$

with $x \in \{0, \dots, d_i - 1\}$ and $y \in \{0, \dots, d_j - 1\}$.

The set E describes an n -vertex-connected graph. Let $\tilde{E} \subseteq E$ defines an n -vertex connected *tree* (acyclic graph). The main result is: the n -qubit Toffoli gate can be achieved with less number of operations if

$$d_i \geq k_i + 1, \quad (60)$$

where d_i is the dimension of a qudit and the number k_i is the qudit's connections to other qudits within \tilde{E} . With this condition fulfilled, the n -qubit Toffoli gate can be realized by $2n - 3$ two-qudit CZ gates. The detailed realization of the n -qubit Toffoli gate by the properties and special operations of the tree in topology can be found in Ref. [22]. The advantage of this scheme is the scalability and the ability to implement it for the multi-qubit controlled unitary gate $C^n U^{(t)}$.

These $C^n U$ gates are a crucial component in the PEA which has many important applications such as the quantum simulation [65] and the Shor's factoring algorithm [66]. This idea of combining qudits of different dimensions or hybrid qudit gates can also be applied to other qudit gates such as the SWAP and SUM gates as shown in Ref. [19, 67]. Thus, introducing qudits into qubit systems to create a hybrid qudit system offers the potential of improvement to quantum computation.

2.2.4 Qudit multi-level controlled gate

For a qubit controlled gate, the control qubit has only two states so it is a “do-or-don’t” gate. Qudits, on the other hand, have multiple accessible states and thus a qudit-controlled gate can perform a more complicated operation [68]. The *Muthukrishan-Stroud gate* (MS gate) for a qudit applies the specified operation on the target qudit only if the control qudit is in a selected one of the d states, and leaves the target unchanged if the control qudit is in any other $d - 1$ states. Hence, the MS gate is essentially a ”do-or-don’t” gate generalized to qudits and does not fully utilize the d states on the control qudit [37].

To fully utilize the d states on the control qudit, people have developed the quantum multiplexer to perform the controlled U operations in a qudit system as shown in Fig. 7, where the MS gate and shifting gates are combined to apply different operations to the target depending on different states on the control states [69]. Here we introduce the *multi-value-controlled gate* (*MVCG*) for qudits, which applies a unique operation to the target qudit for each unique state of the control qudit [2].

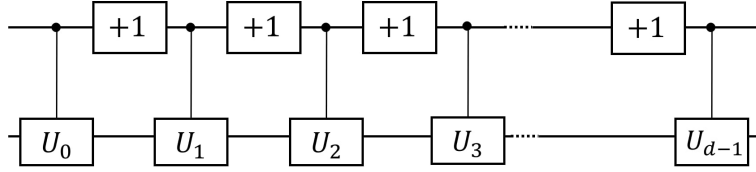


Figure 7: d -valued Quantum Multiplexer for the second qudit and its realization in terms of Muthukrishan-Stroud gates (the control U operation that only act on one specific control state). The gate labeled $+1$ is the shifting gate that increases the state value of the control qudit by $1 \pmod{d}$. Depending on the value of the top control qudit, one of U_i is applied to the second qudit, for $i \in \{0, 1, \dots, d - 1\}$.

For a d -dimensional qudit system, a two-qudit multi-value-controlled gate is represented by a $d^2 \times d^2$ matrix

$$MVCG = \begin{pmatrix} U_0 & 0 & 0 & \cdots & 0 \\ 0 & U_1 & 0 & \cdots & 0 \\ 0 & 0 & U_2 & \cdots & 0 \\ \vdots & \vdots & \vdots & \ddots & \vdots \\ 0 & 0 & 0 & \cdots & U_{d-1} \end{pmatrix}, \quad (61)$$

where each U_i ($i = 0, 1, \dots, d - 1$) is a unique unitary single-qudit operation. The U_i operation is applied to the target qudit when the control qudit is in $|i\rangle$ state. In the later sections, §3.2.1 and §3.2.2 the controlled gates are *MVCG* and improve the efficiency of the qudit algorithm. *MVCG* can be built in many physical systems and one example in a photonic system is introduced in §4.1.

2.3 Geometrically quantifying qudit-gate efficiency

In a quantum computer, each qudit can remain coherent for a limited amount of time (decoherence time). After this time, the quantum information is lost due to the outside perturbations and noises. In the computation process, quantum gates take certain amount of time to alter the states of the qudits. The decoherence time of a qudit state limits the number of quantum gates in the circuit. Therefore, we need to design more efficient algorithms and circuits. A method exists to do a general systematic evaluation of the circuit efficiency with the mathematical techniques of Riemannian geometry [70]. By reforming the quantum circuits designing problems as a geometric problem, we are able to develop new quantum algorithms or to exploring and evaluating the full potential of the quantum computers. This evaluation is able to generalized to qutrit systems, where the least amount of the gates required to synthesize any unitary operation is given [4].

To begin with, we assume that the operations done by the quantum circuit can be described by a unitary evolution U derived from the time-dependent Schrödinger equation $dU/dt = -iHU$ with the boundary condition t_f , $U(t_f) = U$. The complexity of realizing U can be characterized by a cost function $F[H(t)]$ on the Hamiltonian control $H(t)$. This allow us to define a Riemannian geometry on the space of unitary operations [71]. Finding the minimal geodesics of this Riemannian geometry is equivalent to finding the optimal control function $H(t)$ of synthesizing the desired U .

Now we transform the problem of calculating a lower bound to the gate number to finding the minimal geodesic distance between the identity operation I and U . Instead of Pauli matrices for the qubit representation of the Hamiltonian, the qutrit version of Hamiltonian is expanded in terms of the Gell-Mann matrices. Here we give an explicit form of the Gell-Mann matrices representation in d -dimension [5] which is used for qutrit (where $d = 3$) as well as other qudit systems in the later part of the section. Let e_{jk} denote the $d \times d$ matrix with a 1 in the (j, k) elements and 0s elsewhere, a basis can be described as

$$u_{jk}^d = e_{jk} + e_{kj}, 1 \leq j < k \leq d, \quad (62)$$

$$u_{jk}^d = i(e_{jk} - e_{kj}), 1 \leq k < j \leq d, \quad (63)$$

$$u_{jj}^d = \text{diag}(1, \dots, 1, -j, 0_{d-2j}), j \in [d-1]. \quad (64)$$

Here, diag represents the diagonal matrix, 0_{d-2j} denotes the zeros of length $d-2j$. u_{jk}^d are traceless and Hermitian and together with the identity matrix $\mathbb{1}_d$ serve as the basis of the vector space of $d \times d$ Hermitian matrix. These generalized Gell-Mann matrices can be used to generate the group representation of $SU(d)$ while the other representations can be achieved by transform these matrices uniformly. To derive the bases of $SU(d^n)$, we first define $x_l = u_{jk}^d$ with $l = jd + k, l \in [d^2]$ and

$$X_l^s = \mathbb{I}^{\otimes s-1} \otimes x_l \otimes I^{\otimes d-s} \quad (65)$$

acts on the s -th qudit with x_l and leaves the other qudits unchanged. The bases of $SU(d^n)$ is constructed by $\{Y_t^{P_t}\}, t \in [n], P_t = \{i_1, \dots, i_t\}$ with all possible

$1 < i_1 < \dots < i_k < n$, where

$$Y_t^P = \prod_{k=1}^t X_{j_k}^{i_k}. \quad (66)$$

Y_t^P denotes all operators with generalized Gell-Mann matrices x_{j_1}, \dots, x_{j_k} acting on t qudits at sites $P = \{i_1, \dots, i_k\}$, respectively, and rest with identity. It is easy to prove that with the generalized Gell-Mann matrices representations, 1-body and 2-body interactions can generate all 3-body interactions.

Now the Hamiltonian in terms of the Gell-Mann matrices (with the notation σ) can be written as

$$H = \sum_{\sigma}^{\prime} h_{\sigma} \sigma + \sum_{\sigma}^{\prime\prime} h_{\sigma} \sigma. \quad (67)$$

All coefficients h_{σ} are real and, in $\sum_{\sigma}^{\prime} h_{\sigma} \sigma$, σ goes over all possible one- and two-body interactions whereas, in $\sum_{\sigma}^{\prime\prime} h_{\sigma} \sigma$, σ goes over everything else. The cost function is

$$F(H) := \sqrt{\sum_{\sigma}^{\prime} h_{\sigma}^2 \sigma + p^2 \sum_{\sigma}^{\prime\prime} h_{\sigma}^2 \sigma}, \quad (68)$$

where p is a penalty cost by applying many-body terms. Now that the control cost is well defined, it is natural to form the distance in the space $SU(3^n)$ of n -qudit unitary operators with unit determinant. We can treat the function $F(H)$ as the norm related to a Riemannian metric with a metric tensor g as:

$$g = \begin{cases} 0, & \sigma \neq \tau \\ 1, & \sigma = \tau \text{ and } \sigma \text{ is one or two body} \\ p^2, & \sigma = \tau \text{ and } \sigma \text{ is three or more body} \end{cases}. \quad (69)$$

The distance $d(I, U)$ between I and U which is the minimum curve connecting I and U equals to the minimal length solution to the geodesic equation

$$\left\langle \frac{dH}{dt}, K \right\rangle = i \langle H, [H, K] \rangle, \quad (70)$$

where $\langle \cdot, \cdot \rangle$ denotes the inner product on the tangent space $SU(3^n)$ defined by the metric components (69), and $[\cdot, \cdot]$ denotes the matrix commutator and K is an arbitrary operator in $SU(3^n)$.

All lemmas backing up the final theorem have been proven in detail [4], but the reasoning behind can be summarized in four parts. First let p be the three- and more-body items penalty. With large enough p , the distance $d(I, U)$ is guaranteed to have a supremum that does not depend on p . Secondly, we have

$$\|U - U_P\| \leq 3^n d([U])/p, \quad (71)$$

where $\|\bullet\|$ is the operator norm and U_P the corresponding unitary operator generated by the one- and two-body items projected Hamiltonian $H_P(t)$. Thirdly,

given an n -qutrit unitary operator U generated by $H(t)$ with the condition $\|H(t)\| \leq c$ in a time interval $[0, \Delta]$, then

$$\|U - \exp(-i\bar{H})\Delta\| \leq 2(e^{c\Delta} - 1 - c\Delta) = O(c^2\Delta^2), \quad (72)$$

where \bar{H} is the mean Hamiltonian. Lastly, for H as an n -qutrit one- and two-body Hamiltonian, a unitary operator U_A exists that satisfies

$$\|e^{iH\Delta} - U_A\| \leq c_2 n^2 \Delta^3 \quad (73)$$

and can be generated with at most $c_1 n^2 / \Delta$ one- and two-qutrit gates, and constants c_1 and c_2 .

All these lemmas combined gives the final theorem for the qutrit system: for a unitary operator U in $SU(3^n)$, $O(n^k d(I, U)^3)$ one- and two-qutrit gates is the lower bound to synthesize a unitary U_A with the condition $|U - U_A| \leq c$, given a constant c . It is worth mentioning that for any groups of unitaries U , which is labeled by the number of qudits n , the final theorem shows a quantum circuit exists with a polynomial of $d(I, U)$ number of gates such that it can approximate U to arbitrary accuracy. Alternatively, a polynomial-sized quantum circuit exists if and only if the distance $d(I, U)$ itself is scaling polynomially with n .

With appropriate modification, the Riemannian geometry method can be used to ascertain the circuit-complexity bound for a qudit system [5]. In this scheme, the unitary matrix $U \in SU(d^n)$ is represented by the generalized Gell-Mann matrices as defined in the earlier part of the section. The main theorem in the qudit case is: “for any small constant ε , each unitary $U_A \in SU(d^n)$ can be synthesized using $O(\varepsilon^{-2})$ one- and two-qudit gates, with error $\|U - U_A\| \leq \varepsilon$.” [5] To break up the constant ε to an explicit form, we have $\varepsilon^{-2} = N^2 d^4 n^2$, where d is the dimension of the qudit, n is the number of qudits and N is the number of the intervals that $d(I, U)$ divides into, such that a small $\delta = d(I, U)/N \leq \varepsilon$. The qudit case shows the explicit relation between the non-local quantum gate cost and the approximation error for synthesizing quantum qudit operations. In summary, for the quantum circuit model, one can decide a lower bound for the number of gates needed to synthesize U by finding the shortest geodesic curve linking I and U . This provides a good reference for the design of the quantum circuit using qudits.

3 Quantum algorithms using qudits

A qudit, with its multi-dimensional nature, is able to store and process a larger amount of information than a qubit. Some of the algorithms described in this section can be treated as direct generalizations of their qubit counterparts and some utilize the multi-dimensional nature of the qudit at the key subroutine of the process. This section introduces examples of the well-known quantum algorithms based on qudits and divides them into two groups: algorithms for the oracle-decision problems in §3.1 and algorithms for the hidden Abelian subgroup problems in §3.2. Finally, §3.3 discusses how the qudit gates can improve

the efficiency of the quantum search algorithm and reduce the difficulty in its physical set-up.

3.1 Qudit oracle-decision algorithm

In this subsection we explore the qudit generalizations of the efficient algorithms for solving the oracle decision problems, which are quite important historically and used to demonstrate the classical-quantum complexity separation [72, 73]. The oracle decision problems is to locate the contents we want from one of the two mutually disjoint sets that is given. We start in §3.1.1 with a discussion about a single-qudit algorithm that determines the parity of a permutation. In §3.1.2, the Deutsch-Jozsa algorithm in qudit system is discussed and its unique extension, the Bernstein-Vazirani algorithm is provided in §3.1.3.

3.1.1 Parity determining algorithm

In this section we review a single qudit algorithm which provides a two to one speedup than the classical counterpart. This algorithm can also be generalized to work on an arbitrary d -dimensional qudit which solves the same problem of a larger computational space [16]. In quantum computing, superposition, entanglement and discord are three important parts for the power of quantum algorithms and yet the full picture behind this power is not completely clear [74].

Recent research shows that we can have a speedup in a fault tolerant quantum computation mode using the quantum contextuality [75]. The contextual nature can be explained as “a particular outcome of a measurement cannot reveal the pre-existing definite value of some underlying hidden variable” [76, 77]. In other words, the results of measurements can depend on how we made the measurement, or what combination of measurements we chose to do. For the qudit algorithm discussed below, a contextual system without any quantum entanglement is shown to solve a problem faster than the classical methods. [16]. Because this qudit algorithm uses a single qudit throughout the process without utilizing any correlation of quantum or classical nature, it acts as a perfect example to study the sources of the quantum speed-up other than the quantum correlation.

The algorithm solves a black-box problems that maps d inputs to d outputs after a permutation. Consider the case of three objects where six possible permutations can be divided into two groups: *even* permutation that is a cyclic change of the elements and *odd* permutation that is an interchange between two elements. If we define a function $f(x)$ that represents the permutation on the set $x \in \{-1, 0, 1\}$, the problems become determining the parity of the bijection $f : -1, 0, 1 \rightarrow -1, 0, 1$. We use Cauchy’s two-line notation to define three possible even functions f_k , namely,

$$f_1 := \begin{pmatrix} 1 & 0 & -1 \\ 1 & 0 & -1 \end{pmatrix}, f_2 := \begin{pmatrix} 1 & 0 & -1 \\ 0 & -1 & 1 \end{pmatrix}, f_3 := \begin{pmatrix} 1 & 0 & -1 \\ -1 & 1 & 0 \end{pmatrix}, \quad (74)$$

and the remaining three odd function are

$$f_4 := \begin{pmatrix} 1 & 0 & -1 \\ -1 & 0 & 1 \end{pmatrix}, f_5 := \begin{pmatrix} 1 & 0 & -1 \\ 0 & 1 & -1 \end{pmatrix}, f_6 := \begin{pmatrix} 1 & 0 & -1 \\ 1 & -1 & 0 \end{pmatrix}. \quad (75)$$

The circuit for the single qutrit algorithm in a space spanned by $\{|1\rangle, |0\rangle, |-1\rangle\}$ is shown in Fig. 8, where the operation U_{f_k} applies f_k to the state: $U_{f_k}(|1\rangle + |0\rangle + |-1\rangle) = |f_k(1)\rangle + |f_k(0)\rangle + |f_k(-1)\rangle$, and FT is the single-qutrit Fourier transform

$$FT = \frac{1}{\sqrt{3}} \begin{pmatrix} \omega & 1 & \omega^{-1} \\ 1 & 1 & 1 \\ \omega^{-1} & 1 & \omega \end{pmatrix} \quad (76)$$

using ω as the cube root of unity (14). The process starts with state $|1\rangle$ undergoing FT and becoming $|\psi_1\rangle$ as $FT|1\rangle = |\psi_1\rangle = \omega|1\rangle + |0\rangle + \omega^{-1}|-1\rangle$. Then we obtain $|\psi_k\rangle$ by applying U_{f_k} to $|\psi_1\rangle$. It is easy to show that

$$|\psi_1\rangle = \omega^{-1}|\psi_2\rangle = \omega|\psi_3\rangle \quad (77)$$

and, similarly,

$$|\psi_4\rangle = \omega^{-1}|\psi_5\rangle = \omega|\psi_6\rangle. \quad (78)$$

Hence, application of U_{f_k} on $|\psi_1\rangle$ gives $|\psi_1\rangle$ (up to a phase factor) for an even permutation and $|\psi_4\rangle = FT|-1\rangle$ for an odd permutation. Thus, applying inverse Fourier transform FT^{-1} at the end, we measure $|1\rangle$ for even f_k and $|-1\rangle$ for odd f_k . We are able to determine the parity of f_k by a single application of f_k on a single qutrit.

Generalizing to a d dimensional qudit system,

$$|\psi_k\rangle := \frac{1}{\sqrt{d}} \sum_{k'=1}^d \omega^{(k'-1)(k-1)} |k'\rangle. \quad (79)$$

In this scenario, a positive cyclic permutation maps $|\psi_2\rangle$ onto itself whereas negative permutations give $|\psi_d\rangle$. We then measure the results after applying an inverse Fourier transform to solve for the parity of the permutation. This algorithm has been implemented on the NMR system for both the qutrit [15] and ququart [16] cases. It is also realized on a linear optic system [78]. Although the model problem has no significant applications and the speedup in the higher dimensional cases is not exponential, this proposed algorithm provides an elegant yet simple example for quantum computation without entanglement.

3.1.2 Qudit Deutsch-Jozsa algorithm

Deutsch algorithm (with its origin in [72] and improved in [67]) is one of the simplest examples to show the speed advantage of quantum computation. Deutsch-Jozsa algorithm is n -qubits generalization of the Deutsch algorithm. Deutsch-Jozsa algorithm can determine if a function $f(x)$ is *constant*, with constant output, or *balanced*, that gives equal instances of both outputs [64]. The process itself consists of only one evaluation of the function $f(x)$. In this algorithm,

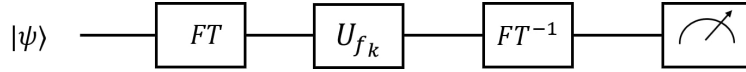


Figure 8: Schematic view of the quantum circuit for the parity determining algorithm. FT is the Fourier transform and U_{f_k} is the gate that does one of the two permutations and the last box represents the measurement.

Alice sends Bob N qubits in the query register and one in the answer register where Bob applies the function to the query register qubits and stores the results in the answer register. Alice can measure the qubits in the query register to determine whether Bob's function is constant or balanced. This algorithm makes use of the superposition property of the qubit and reduces the minimum number of the function call from $2^n/2 + 1$ classically to only 1 with quantum algorithm. This gives another example of the advantages of quantum algorithms.

The Deutsch-Jozsa algorithm can be performed in the qudit system with a similar setup. Furthermore, with the qudit system, Deutsch-Jozsa algorithm can also find the closed expression of an affine function accurate to a constant term [79]. The *constant* and *balanced* function in the n dimensional qudit case have the following definition: "An r -qudit multi-valued function of the form

$$f : \{0, 1, \dots, n-1\}^r \rightarrow \{0, 1, \dots, n-1\} \quad (80)$$

is *constant* when $f(x) = f(y) \forall x, y \in \{0, 1, \dots, n-1\}^r$ and is *balanced* when an equal number of the n^r domain values, namely n^{r-1} , is mapped to each of the n elements in the co-domain" [79].

It can be shown that all of the affine functions of r qudits

$$f(x_1, \dots, x_r) := A_0 \oplus A_1 x_1 \oplus \dots \oplus A_r x_r, \quad A_0, \dots, A_r \in \mathbb{Z}_n, \quad (81)$$

can be categorized to either constant or balanced functions [79]. If all the coefficients $A_{i \neq 0} = 0$ then the function is constant. For affine function with non-zero coefficient $A_{i \neq 0}$, every element in its domain $\{0, 1, \dots, n-1\}^r$ is reducible modulo n to a unique element $m \in \{0, 1, \dots, n-1\}$. As $f(p) = f(q)$ if $p \equiv q \pmod{n}$, each of the elements in the codomain $\{0, 1, \dots, n-1\}$ is mapped to n^{r-1} different elements in the domain. To finish the proof of the n -nary Deutsch-Jozsa algorithm, another trivial lemma is needed: Primitive n^{th} roots of unity satisfy $\sum_{k=0}^{n-1} \omega^{\alpha k} = 0$ for nonzero integers α .

The circuit of the Deutsch-Jozsa algorithm in qudits is shown in Fig. 9. This algorithm of r qudits can both distinguish whether a function U_f is balanced or constant and verify a closed expression for an affine function in U_f within a constant term which is a universal phase factor of the x -register and thus is lost during the measurement. The other coefficients of the affine function A_1, \dots, A_r are determined by measuring the state of the x -register at the output, $|A_1, \dots, A_r\rangle$.

A detailed derivation of the circuit has been shown [79], but the reasoning is an analogy to the qubit version of the Deutsch-Jozsa algorithm. If the function

U_f is constant, the final state after the measurement is $|0\rangle^{\otimes r} |n-1\rangle$ as for $j \neq 0$ every states in the x -register have null amplitudes. Therefore, if every x -register qudit yields $|0\rangle$, it is a constant function; otherwise the function is balanced.

The Deutsch-Jozsa algorithm in the qudit system shares the same idea while enabling more applications such as determining the closed form of an affine function. Although this algorithm is mainly of theoretical interest, the n -ary version of it may have applications in image processing. It has the potential to distinguish between maps of texture in a Marquand chart since the images of which are encoded by affine functions [23]. This algorithm can also be modified to set up a secure quantum key-distribution protocol [23]. Other proposed Deutsch-Jozsa algorithms exist such as a method that makes use of the artificially allocated subsystems as qudits [80] and a generalized algorithm on the virtual spin representation [81].

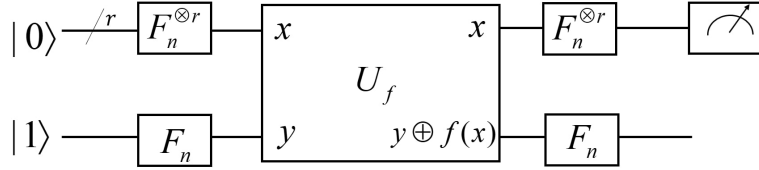


Figure 9: The Deutsch-Jozsa circuit in qudit system. The F_n are the qudit Hadamard gates achieved with quantum Fourier transform.

3.1.3 Qudit generalization of the Bernstein-Vazirani algorithm

in §3.1.2 we have discussed an application of a qudit Deutsch-Jozsa algorithm (DJA): verify a closed expression of an affine function. This application is closely related to the Bernstein-Vazirani algorithm discussed in this section. Given an input string and a function that calculates the bit-wise inner-product of the input string with an unknown string, the Bernstein-Vazirani algorithm determines the unknown string [82]. This algorithm can be treated as an extension of the Deutsch-Jozsa algorithm.

The qudit generalization of the BernsteinVazirani algorithm can determine a number string of integers modulo d encoded in the oracle function [83, 24]. First we introduce a positive integer d and consider the problem in modulo d throughout. Given an N -component natural number string

$$g(a) := (g(a_1), g(a_2), g(a_3), \dots, g(a_N)), \quad g(a_j) \in \{0, 1, \dots, d-1\}, \quad (82)$$

we define

$$f(x) := g(a) \cdot x \quad \text{mod } d = g(a_1)x_1 + g(a_2)x_2 + \dots + g(a_N)x_N \quad \text{mod } d, \quad (83)$$

for

$$x = (x_1, x_2, \dots, x_N) \in \{0, 1, \dots, d-1\}^N. \quad (84)$$

The oracle in the algorithm applies $f(x)$ to the input string x and computes the result, namely, the number string $g(a)$ encoded in the function $f(x)$.

The input state x is chosen to be $|\psi_0\rangle = |0\rangle \otimes^N |d-1\rangle$, where $|0\rangle \otimes^N$ means initialization of the N control-qudits into their $|0\rangle$ states and $|d-1\rangle$ means the target qudit is in its $d-1$ state. Quantum Fourier transforms of the pertinent input states are

$$|0\rangle \xrightarrow{QFT} \sum_{y=0}^{d-1} \frac{|y\rangle}{\sqrt{d}} |d-1\rangle \xrightarrow{QFT} \sum_{y=0}^{d-1} \frac{1}{\sqrt{d}} \omega^{d-y} |y\rangle, \quad (85)$$

for ω a root of unity (14). The component-wise Fourier transform of a string encoded in the state $|x_1 x_2 \dots x_N\rangle$ is

$$|x_1 x_2 \dots x_N\rangle \xrightarrow{QFT} \sum_{z \in K} \frac{\omega^{x \cdot z} |z\rangle}{\sqrt{d^N}}, \quad (86)$$

where

$$K = \{0, 1, \dots, d-1\}^N, \quad z := (z_1, z_2, \dots, z_N). \quad (87)$$

We denote the Fourier transform of the $|d-1\rangle$ state as $|\phi\rangle$ and the input state after the Fourier transform is

$$|\psi_1\rangle = \sum_{z \in K} \frac{|x\rangle}{\sqrt{d^N}} |\phi\rangle \quad (88)$$

Now we introduce the oracle as the $O_{f(x)}$ gate such that

$$|x\rangle |j\rangle \xrightarrow{O_{f(x)}} |x\rangle |(f(x) + j) \bmod d\rangle, \quad (89)$$

where

$$f(x) = g(a) \cdot x \bmod d. \quad (90)$$

By applying the $O_{f(x)}$ gate to $|\psi_1\rangle$ and following the formula by phase kick-back, we obtain the output state

$$O_{f(x)} |\psi_1\rangle = |\psi_2\rangle = \sum_{z \in K} \frac{\omega^{f(x)} |x\rangle}{\sqrt{d^N}} |\phi\rangle. \quad (91)$$

Finally, obtain the $|\psi_3\rangle$ which is the state after inverse Fourier transform of the first N qudits of $|\psi_2\rangle$. By measuring the first N quantum state of $|\psi_3\rangle$ we can obtain the natural number string we want that is offset up to a constant

$$g(a_1), g(a_2), g(a_3), \dots, g(a_N) \quad (92)$$

using a single query of the oracle function.

The Bernstein-Vazirani algorithm clearly demonstrates the power of quantum computing. It outperforms the best classical algorithm in terms of speed by a factor of N [83]. The qudit generalizations of the Bernstein-Vazirani algorithm helps us comprehend the potential of the qudit systems.

3.2 Qudit algorithms for the hidden Abelian subgroup problems.

Many of the widely used quantum algorithms such as the discrete Fourier transform, the phase estimation and the factoring fit into the framework of the hidden subgroup problem (HSP). In this section, we review the qudit generalization of these algorithms. The qudit Fourier transform is discussed in §3.2.1 and its application, the PEA is reviewed in §3.2.2. A direct application of these algorithms, the Shor's factoring algorithm performed with qutrits and in metaplectic quantum architectures is also introduced §3.2.2.

3.2.1 Quantum Fourier Transform with qudits

The quantum Fourier transform algorithm (QFT) is realizable on a qubit system [64]. QFT, as the heart of many quantum algorithms, can also be performed in a qudit system [60, 84]. In an N -dimensional system represented with n d -dimensional qudits, the QFT, $F(d, N)$, where $N = d^n$, transforms the computational basis

$$\{|0\rangle, |1\rangle, \dots, |n-1\rangle\} \quad (93)$$

into a new basis set [25]

$$F(d, N) |j\rangle = \frac{1}{\sqrt{N}} \sum_{k=0}^{N-1} e^{2\pi i j k / N} |k\rangle. \quad (94)$$

For convenience, we write an integer j in a base- d form. If $j > 1$ then

$$j = j_1 j_2 \cdots j_n = j_1 d^{n-1} + j_2 d^{n-2} + \cdots + j_n d^0 \quad (95)$$

and, if $j < 1$, then

$$j = 0.j_1 j_2 \cdots j_n = j_1 d^{-1} + j_2 d^{-2} + \cdots + j_n d^{-n}. \quad (96)$$

The QFT acting on a state $|j\rangle$ can be derived and rewritten in a product form as

$$\begin{aligned} |j\rangle = |j_1 j_2 \cdots j_n\rangle &\mapsto \frac{1}{d^{n/2}} \sum_{k=0}^{d^n-1} e^{2\pi i j k / d^n} |k\rangle \\ &= \frac{1}{d^{n/2}} \sum_{k_1=0}^{d-1} \cdots \sum_{k_n=0}^{d-1} e^{2\pi i j (\sum_{l=1}^n k_l d^{-l})} |k_1 k_2 \cdots k_n\rangle \\ &= \frac{1}{d^{n/2}} \sum_{k_1=0}^{d-1} \cdots \sum_{k_n=0}^{d-1} \bigotimes_{l=1}^n e^{2\pi i j k_l d^{-l}} |k_l\rangle \\ &= \frac{1}{d^{n/2}} \bigotimes_{l=1}^n \left[\sum_{k_l=0}^{d-1} e^{2\pi i j k_l d^{-l}} |k_l\rangle \right]. \end{aligned}$$

This process can be realized with the quantum circuit shown in Fig. 10, and the fully expanded expression of the product form is shown on the right side of the figure. The generalized Hadamard gate H^d in the figure is defined as $H^d := F(d, d)$ which effects the transform

$$H^d |j_n\rangle = |0\rangle + e^{2\pi i 0 \cdot j_n} |1\rangle + \dots + e^{2(d-1)\pi i 0 \cdot j_n} |d-1\rangle. \quad (97)$$

The matrix representation of H^d is

$$\begin{pmatrix} 1 & 1 & \dots & 1 \\ 1 & e^{2\pi i 0 \cdot 1} & \dots & e^{2\pi i 0 \cdot (d-1)} \\ \vdots & \vdots & \ddots & \vdots \\ 1 & e^{2(d-1)\pi i 0 \cdot 1} & \dots & e^{2(d-1)\pi i 0 \cdot (d-1)} \end{pmatrix}. \quad (98)$$

In the circuit the R_k^d gate is a phase gate that has the expression

$$R_k^d = \begin{pmatrix} 1 & 0 & \dots & 0 \\ 0 & e^{2\pi i / d^k} & \dots & 0 \\ \vdots & \vdots & \ddots & \vdots \\ 0 & 0 & \dots & e^{2\pi i (d-1) / d^k} \end{pmatrix}. \quad (99)$$

The black dots in the circuit are multi-value-controlled gates that apply R_k^d to the target qudit j times for a control qudit in state $|j\rangle$. A straightforward derivation shows that the circuit produces the results on the left side of the figure. In order to complete the Fourier transform and ensure the correct sequence of $j_1 j_2 \dots j_n$, a series of SWAP gates are applied at the end, which are not explicitly drawn in Fig. 10.

The QFT developed in qudit system offers a crucial subroutine for many quantum algorithm using qudits. Qudit QFT offers superior approximations where the magnitude of the error decreases exponentially with d and the smaller error bounds are smaller [84], which outperforms the binary case [85].

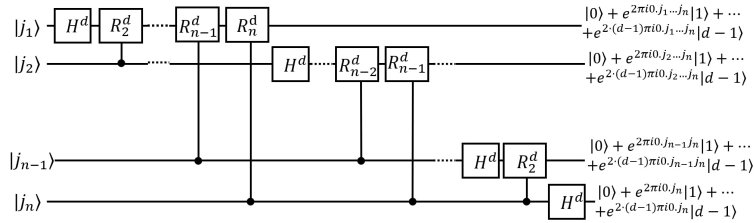


Figure 10: Quantum Fourier transform in qudit system. H^d is the d -dimensional Hadamard gate and the expression of the R^d gate is shown in Eq. (99). Resultant states are shown to the right.

3.2.2 Phase-estimation algorithm with qudits

With the qudit quantum Fourier transform, we are able to generalize the PEA to qudit circuits [25]. Similar to the PEA using qubit, the PEA in the qudit system is composed by two registers of qudits. The first register contains t qudits and t depends on the accuracy we want for the estimation. We assume that we can perform a unitary operation U to an arbitrary number of times using qudit gates and generate its eigenvector $|u\rangle$ and store it using the second register's qudits [26]. We want to calculate the eigenvalue of $|u\rangle$ where $U|u\rangle = e^{2\pi ir}|u\rangle$ by estimating the phase factor r .

The following derivations follow those in Ref. [25]. For convenience, we rewrite the rational number r as

$$r = R/d^t = \sum_{l=1}^t \bar{R}_l/d^l = 0.\bar{R}_1\bar{R}_2\cdots\bar{R}_t. \quad (100)$$

As shown in Fig. 11, each qudit in the first register passes through the generalized Hadamard gate $H \equiv F(d, d)$. For the l^{th} qudit of the first register, we have

$$F(d, d) |0\rangle_l = \frac{1}{\sqrt{d}} \sum_{k_l=0}^{d-1} |k_l\rangle. \quad (101)$$

Then the l^{th} qudit is used to control the operation $U^{d^{t-l}}$ on the target qudits of the state $|u\rangle$ in the second register, which gives

$$CU^{d^{t-1}} |k\rangle \otimes |u\rangle = |k\rangle (U^{d^{t-1}})^k |u\rangle = e^{2\pi i k d^{t-1} r} |k\rangle \otimes |u\rangle. \quad (102)$$

Note that the function of the controlled operation $CU^{d^{t-1}}$ can be considered as a 'quantum multiplexer' [32, 86, 69]. After executing all the controlled operations on the qudits, the qudit system state turns out to be

$$\left(\prod_{l=1}^t \otimes \frac{1}{\sqrt{d}} \sum_{k_l=0}^{d-1} e^{2\pi i k_l d^{t-l} r} |k_l\rangle \right) \otimes |u\rangle. \quad (103)$$

Therefore, through a process called the "phase kick-back", the state of the first register receives the phase factor and becomes

$$|\text{Register 1}\rangle = \frac{1}{d^{t/2}} \sum_{k=0}^{d^t-1} e^{2\pi i r k} |k\rangle. \quad (104)$$

The eigenvalue r which is represented by the state $|R\rangle$ can be derived by applying the inverse QFT to the qudits in the first register:

$$F^{-1}(d, d^t) |\text{Register 1}\rangle = |R\rangle. \quad (105)$$

The whole process of PEA is shown in Fig. 12. To obtain the phase $r = R/d^t$ exactly, we can measure the state of the first register in the computational basis.

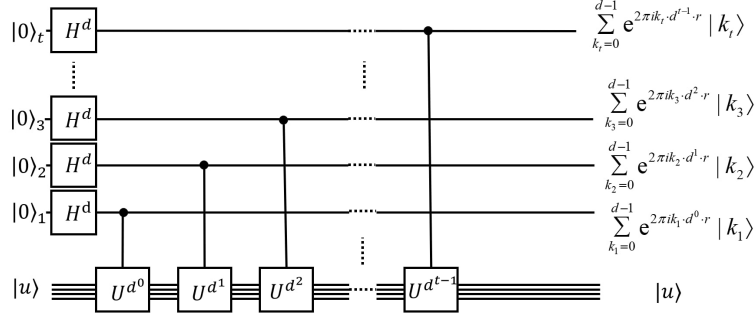


Figure 11: The circuit for the first stage of the PEA. The qudits in the second register whose states represent $|u\rangle$ are undergoing the U operations and the generated phase factors are kicking back to the qudits in the first register, giving the results to the right.

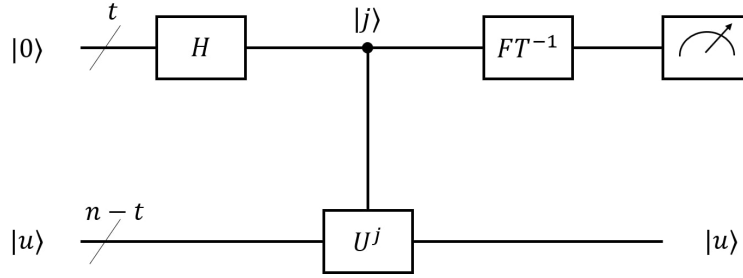


Figure 12: The schematic circuit for the whole stage of PEA. After the first stage of the PEA, inverse Fourier transform(FT^{-1}) is applied to the qudits in the first register and the phase factors can be obtained by measuring the states of the first register qudits.

The PEA in qudit system provides a significant improvement in the number of the required qudits and the error rate decreases exponentially as the qudit dimension increases [87]. A long list of PEA applications includes the Shor's factorization algorithm [66], simulation of quantum systems [88], solving linear equations [89, 90], and quantum counting [91]. To give some examples, a quantum simulator utilizing the PEA algorithm has been used to calculate the molecular ground-state energies [65] and to obtain the energy spectra of molecular systems [92, 93, 94, 95, 96]. Recently, a method to solve the linear system using a qutrit version of the PEA has been proposed [97]. The qudit version of the PEA opens the possibility to realize all those applications that have the potential to out-perform their qubit counterparts.

The Shor's quantum algorithm for prime factorization gives an important

example of super-polynomial speed-up offered by a quantum algorithm over the currently-available classical algorithms for the same purpose [98]. The order-finding algorithm at the core of the factoring algorithm is a direct application of the PEA. With the previous discussion on the qudit versions of the quantum Fourier transform and phase estimation, we have the foundation to generalize the Shor’s factoring algorithm to the higher dimensional qudit system. Several proposals for performing the Shor’s algorithm on the qudit system, such as the adiabatic quantum algorithm of two qudits for factorization [6], exist. This method makes use of a time-dependent effective Hamiltonian in the form of a sequence of rotation operators that are selected according to the qudit’s transitions between its neighboring levels.

Another proposal carries out a computational resource analysis on two quantum ternary platforms [26]. One is the “generic” platform that uses magic state distillation for universality [52]. The other, known as a metaplectic topological quantum computer (MTQC), is a non-Abelian anyonic platform, where the anyonic braiding and interferometric measurement is used to achieve the universality with a relatively low cost [8, 9]. The article discusses two different logical solutions for the Shor’s period-finding function on each of the two platforms: one that encodes the integers with the binary subspace of the ternary state space and optimizes the known binary arithmetic circuits; the other encodes the integer directly in the ternary space using the arithmetic circuits stemming in Ref [10]. Significant advantages for the MTQC platform are found compared to the others. In particular the MTQC platform can factorize an n -bit number with $n + 7$ logical qutrits with the price of a larger circuit-depth. To sum up the comparison, the MTQC provides significant flexibility at the period finding algorithm for the ternary quantum computers.

3.3 Quantum search algorithm with qudits

The quantum search algorithm, also known as the Grover’s algorithm, is one of the most important quantum algorithms that illustrates the advantage of quantum computing. The Grover’s algorithm is able to outperform the classical search algorithm for a large database. The size of the computational space in an n -qubit system is a Hilbert space of 2^n dimensions.

Since there is a practical limit for the number of working qubits, the working Hilbert space can be expanded by increasing the dimension of each carrier of information, i.e., using qudits and qudit gates. Several schemes of Grover’s quantum search with qudits have been proposed, such as one that uses the discrete Fourier transform as an alternative to the Hadamard gate [99] or another d -dimensional transformation [100] for the construction of the reflection-about-average operator (also known as the diffusion operator). In this section, an instruction on setting up the Grover’s algorithm in the qudit system is reviewed as well as a proposal of a new way to build a quantum gate F that can generate an equal-weight superposition state from a single qudit state [27]. With the new gate F , it is easier to realize the Grover’s algorithm in a physical system and improve the overall efficiency of the circuit.

The Grover's algorithm solves the unstructured search problem by applying the Grover's oracle iteratively. To construct the oracle, we build qudit gates to perform the oracle function $f(x)$ that acts differently on the search target s as compared to all the others. The logic behind the algorithm is to amplify the amplitude of the marked state $|s\rangle$ with the oracle function, while attenuating the amplitudes of all the other states. The marked state is amplified enough to be located in $O(\sqrt{N})$ steps for an N dimensional search space. In each step the Grover's oracle is executed one time. This oracle can be broken into two parts: (1) *Oracle query*: the oracle shifts the phase of the marked state $|s\rangle$ and leaving others unchanged by doing

$$\mathbf{R}_s(\phi_s) = \mathbf{1} + (e^{i\phi_s} - 1) |s\rangle \langle s|. \quad (106)$$

(2) *Reflection-about-average*. This operation is a reflection about a vector $|a\rangle$ with a phase ϕ_a :

$$\mathbf{R}_a(\phi_a) = \mathbf{1} + (e^{i\phi_a} - 1) |a\rangle \langle a|. \quad (107)$$

It is constructed by applying the generalized Hadamard gate H , applying phase shift to $|0\rangle$ state and then applying H again. It is straightforward to show that

$$H^{\otimes n} \mathbf{R}_0(\phi_a) H^{\otimes n} = \mathbf{R}_a(\phi_a).$$

The two steps combined form the Grover's operator \mathbf{G} , which is one execute of the Grover's iteration.

Building Grover's operator in a qudit system can be simplified both algorithmically and physically. The most important improvement can be achieved by replacing the Hadamard gate H with F which drives the single-qudit state $|0_k\rangle$ into an equal weight superposition state,

$$F|0_k\rangle = \sum_{q=0}^{d-1} \xi_q |qk\rangle, \quad (108)$$

with $|\xi_q| = d^{-1/2}$, in all qudits ($k \in \{1, 2, \dots, n\}$). The F function can be realized by a single physical interaction in a multipod system easily. The multipod system consists of d degenerate quantum states $|0\rangle, |1\rangle, \dots, |d-1\rangle$. A common (ancilla) state $|c\rangle$ couples these states to each other by two-photon Raman processes, as illustrated in Fig. 13. The root-mean-square (rms) Rabi frequency as the coupling factor of the two states is

$$\Omega(t) = \sqrt{\sum_{k=0}^{d-1} |\Omega_k(t)|^2}. \quad (109)$$

Then from the two-state solution, we can calculate the dynamics of the multipod [101].

This method of building F minimizes the number and the duration of algorithmic steps and thus is fast to implement and, in addition, it also provides

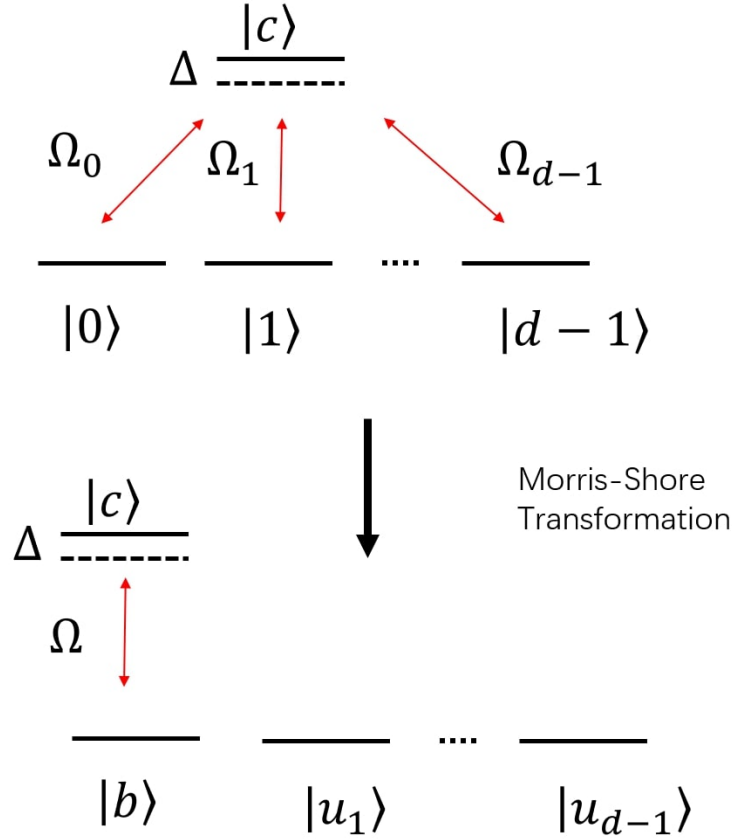


Figure 13: Illustration of a qudit multipod linkage: the top is in the original basis and the bottom is in the Morris-Shore basis. Δ is a common detuning between a common (ancilla) state and other qudit states, Ω_k represents the single-photon Rabi frequencies. State $|b\rangle$ is a superposition of the qudit states weighted by the couplings Ω_k ; $|u_n\rangle$ are the states that are not in the dynamics.

better protection against detrimental effects such as decoherence or imperfections. Due to its conceptual simplicity, this method has applications in numerous physical systems. Thus, it is one of the most natural and simplest realizations of Grover's algorithm in qudits.

4 Implementations of qudits

The qubit circuit and qubit algorithm have been implemented on various physical systems such as defects in solids [102, 103, 104], quantum dots [105, 106],

photons [107, 108], super conducting systems [109, 110], trapped ions [111, 112], magnetic [113, 114, 115, 116] and non-magnetic molecules [117, 118]. For each physical representation of the qubit, only two levels of states are used to store and process quantum information. However, many quantum properties of these physical systems have more than two levels, such as the frequency of the photon [2], energy levels of the trapped ions [14], spin states of the nuclear magnetic resonance systems [15] and the spin state of the molecular magnetic magnets [119]. Therefore, these systems have the potential to represent qudit systems. In this section, we briefly review several physical platforms that have been used to implement qudit gates or qudit algorithms.

Although most of the systems have three or four levels available for computation, they are extensible to higher level systems and scalable to multi-qudit interactions. These pioneer implementations of qudit systems show the potential of future realization of the more powerful qudit quantum computers that have real-life applications.

4.1 Time and frequency bin of a photon

Photonic system is a good candidate for quantum computing because photons rarely interact with other particles and thus have a comparatively long decoherence time. In addition, photon has many quantum properties such as the orbital angular momentum [120, 121], frequency-bin [122, 123, 124, 125] and time-bin [126, 127] that can be used to represent a qudit. Each of these properties provides an extra degrees of freedom for the manipulation and computation. Each degree of freedom usually has dimensions greater than two and thus can be used as a unique qudit. The experimental realization of arbitrary multidimensional multiphotonic transformations has been proposed with the help of ancilla state, which is achievable via the introduction of a new quantum nondemolition measurement and the exploitation of a genuine high-dimensional interferometer [11]. Experimental entanglement of high-dimensional qudits, where multiple high-purity frequency modes of the photons are in a superposition coherently, is also developed and demonstrated. [122].

Here we review a single photon system that has demonstrated a proof-of-principle qutrit PEA [2]. In a photonic system, there is no deterministic way to interact two photons and thus it is hard to build a reliable controlled gate for the photonic qudits. The following photonic system bypasses this difficulty via using the two degrees of freedom on a single photon—i.e., the time-bin and frequency-bin to be the two qutrits. The frequency degree of freedom carries one qutrit as the control register and the time degree of freedom carries another qutrit as the target register. The experimental apparatus consists of the well-established techniques and fiber-optic components: continuous-wave(CW) laser source, phase modulator(PM), pulse shaper(PS), intensity modulator(IM) and chirped fiber Bragg grating(CFBG). The device is divided into three parts [2]: 1. A state preparation part that comprises a PM followed by a PS and a IM that encodes the initial state to qudits; 2. a controlled-gate part that is built with a PM sandwiched by two CFBGs to perform the control- U operation; and

3. an inverse Fourier transformation comprising a PM and then a PS to extract the phase information. Note that the controlled-gate part can perform a multi-value-controlled gate that applies different operations based on the three unique states of the control qutrit. In the PEA procedure, eigenphases can be retrieved with 98% fidelity. In addition to having long coherence lifetime, the photonic system also has a unique advantage over other common quantum devices i.e., the ability to process and measure thousands of photons simultaneously. This allows us to generate statistical patterns quickly and infer the phase accurately whereas the normal PEA has to use additional qudits on the control register to increase accuracy.

\hat{U}_1			
Eigenstate	$ 0\rangle_t$	$ 1\rangle_t$	$ 2\rangle_t$
E_0	$.9948 \pm .0004$	$.0101 \pm .0004$	$.0122 \pm .0005$
E_1	$.0023 \pm .0002$	$.9805 \pm .0009$	$.0120 \pm .0005$
E_2	$.0029 \pm .0002$	$.0094 \pm .0004$	$.9758 \pm .0010$
True Phase, ϕ	0	$2\pi/3$	$4\pi/3$
Est. Phase, $\hat{\phi}$	1.972π	$.612\pi$	1.394π
Error, $\frac{ \phi-\hat{\phi} }{2\pi}$	1.4%	2.7%	3.0%
\hat{U}_2			
Eigenstate	$ 0\rangle_t$	$ 1\rangle_t$	$ 2\rangle_t$
E_0	$.878 \pm .002$	$.316 \pm .003$	$.143 \pm .002$
E_1	$.032 \pm .001$	$.530 \pm .003$	$.318 \pm .003$
E_2	$.090 \pm .002$	$.154 \pm .002$	$.539 \pm .003$
True Phase, ϕ	0	$.3511\pi$	1.045π
Est. Phase, $\hat{\phi}$	1.859π	$.377\pi$	1.045π
Error, $\frac{ \phi-\hat{\phi} }{2\pi}$	7.1%	1.3%	0.0%

Table 1: Normalized photon counts and comparison of the true phase ϕ and the experimentally estimated phase $\hat{\phi}$ for each eigenstate of \hat{U}_1 (Eq. 110) and \hat{U}_2 (Eq. 111) [2].

Here we provide an example for the statistical inference of the phase based on numerical data generated by the photonic PEA experiment just described. The two unitary operations used in the experimental setup are

$$\hat{U}_1 = \text{diag}(1, \omega, \omega^2), \quad (110)$$

with ω being the cube root of unity (14), and

$$\hat{U}_2 = \text{diag}(1, e^{i0.351\pi}, e^{i1.045\pi}). \quad (111)$$

In the experiment, photonic qutrits are sent through the control and target registers and the state of the control register qutrits is measured and counted to obtain the phase information.

Given the eigenphase ϕ of an eigenstate of the target register, the probability for the qutrit output state to fall into $|n\rangle$, where $n \in \{0, 1, 2\}$, is

$$C(n, \phi) = \frac{1}{9} \left| 1 + e^{i(\phi - \frac{n2\pi}{3})} + e^{i2(\phi - \frac{n2\pi}{3})} \right|^2. \quad (112)$$

Now let E_0 , E_1 , and E_2 be the counts of the photons that fell into $|0\rangle_f$, $|1\rangle_f$, and $|2\rangle_f$. The estimated phase, denoted $\tilde{\phi}$, is the phase that has the smallest the mean-square error between the measured and theoretical results:

$$\min_{\tilde{\phi}} \sum_{n=0}^2 (E_n - C(n, \tilde{\phi}))^2 \quad (113)$$

The estimated phases for \hat{U}_1 (110) and \hat{U}_2 (111) are shown in Table 1 [2]. The first experiment with U_1 estimates the phase of a eigenvector and gives the eigenvalue. The second experiment with U_2 estimates the phase of a state with an arbitrary value (not a fraction of π), but, by repeating the experiment, the eigenvalue can be estimated from the statistical distribution of the results.

4.2 Ion trap

Intrinsic spin, an exclusively quantum property, has an inherently finite discrete state space which is a perfect choice for representing qubit or qudit. When a charged particle has spin, it possess a magnetic momentum and is controllable by external electromagnetic pulses. This concept leads to the idea of ion trap where a set of charged ions are confined by electromagnetic field. The hyperfine (nuclear spin) state of an atom, and lowest level vibrational modes (phonons) of the trapped atoms serves as good representations of the qudits. The individual state of an atom is manipulated with laser pulse and the ions interact with each other via a shared phonon state.

The set-up of an ion trap qutrit system reviewed here can perform arbitrary single qutrit gates and a control-not gate [14]. These two kinds of gates form a universal set and thus can be combined to perform various quantum algorithms such as those discussed in §3. The electronic levels of an ion are shown in Fig. 14. The energy levels $|0\rangle$, $|1\rangle$, $|2\rangle$ are used to store the quantum information of a qutrit. To define the conditional two-qutrit gate we need an auxiliary level $|0'\rangle$. The transition between the levels are driven by the classical fields Ω_{03} , Ω_{13} , Ω_{04} and Ω_{24} of the Raman transitions through independent channels linked to orthogonal polarizations. The following expressions follow those in Ref. [14]. For single qutrit gates, where the center-of-mass motion is excluded, and assuming the conditions

$$\Delta = (\omega_4 - \omega_0) - \nu_2 = (\omega_3 - \omega_0) - \nu_2 = (\omega_4 - \omega_2) - \nu_1 = (\omega_3 - \omega_1) - \nu_1 \quad (114)$$

and

$$\Delta \gg \Omega_{04}, \Omega_{03}, \Omega_{31}, \Omega_{42}, \quad (115)$$

the effective Hamiltonian describing the ion is

$$\frac{H}{\hbar} = -\frac{|\Omega_{31}|^2}{\Delta} |1\rangle \langle 1| - \frac{|\Omega_{42}|^2}{\Delta} |2\rangle \langle 2| - \frac{|\Omega_{30}|^2 + |\Omega_{40}|^2}{\Delta} |0\rangle \langle 0| - \quad (116)$$

$$- \left[\frac{\Omega_{31}\Omega_{30}^*}{\Delta} |0\rangle \langle 1| + \frac{\Omega_{42}\Omega_{40}^*}{\Delta} |0\rangle \langle 2| + \text{hc} \right]. \quad (117)$$

The evolution operator in the restricted three-dimensional space spanned by $\{|2\rangle, |1\rangle, |0\rangle\}$ is

$$U(\varphi) = \begin{pmatrix} 1 + |g|^2 C(\varphi) & gg'^* C(\varphi) & -ig \sin \varphi \\ g'g^* C(\varphi) & 1 + |g'|^2 C(\varphi) & -ig' \sin \varphi \\ -ig^* \sin \varphi & -ig'^* \sin \varphi & \cos \varphi \end{pmatrix}, \quad (118)$$

where $\varphi = \Omega t$ represents interaction time and

$$C(\varphi) = \cos \varphi - 1, \quad \Omega^2 = |\kappa'|^2 + |\kappa|^2. \quad (119)$$

The notation g and g' represents

$$g := \kappa/\Omega, \quad g' = \kappa'/\Omega, \quad \kappa := \Omega_{42}^* \Omega_{40}/\Delta, \quad \kappa' = \Omega_{31}^* \Omega_{30}/\Delta. \quad (120)$$

All kinds of transitions can be addressed by manipulating the κ and κ' coupling.

The conditional two-qutrit gate is achievable via the center-of-mass (CM) motion of ions inside the trap. The ion CM coupled to the electronic transition $|0\rangle \rightarrow |q\rangle$ is described by the Hamiltonian

$$H_{n,q} = \frac{\Omega_q \eta}{2} [|q\rangle_n \langle 0| a e^{-i\delta t - i\phi} + a^\dagger |0\rangle_n \langle q| e^{i\delta t + i\phi}]. \quad (121)$$

Here a is the annihilation and a^\dagger is the creation operators of the CM phonons. Ω_q is the effective Rabi frequency after adiabatic elimination of upper excited levels and ϕ is the laser phase, and

$$\delta = \omega_2 - \omega_0 - \nu_2 + \nu_1 + \nu_x = \omega_1 - \omega_0 - \nu_2 + \nu_1 + \nu_x \quad (122)$$

is the detuning. The Lamb-Dicke parameter is

$$\eta := \sqrt{\hbar k_\theta^2 / (2M\nu_x)}. \quad (123)$$

With appropriate selection of effective interaction time and laser polarizations, the CM motion coupled to electronic transitions is coherently manipulated. This Hamiltonian governs coherent interaction between qutrits and collective CM motion.

To complete the universal quantum computation requirements, we need to develop a measurement scheme. In this scheme, von Neumann measurements distinguishing three directions $|0\rangle, |1\rangle, |2\rangle$ are made possible via the resonant interactions from $|1\rangle$ and $|2\rangle$ to states $|3\rangle$ and $|4\rangle$, respectively. The single and two-qutrit controlled gate are combined to perform various qutrit algorithms

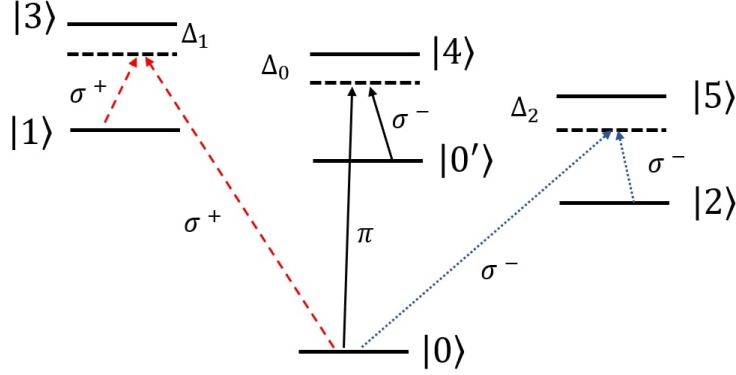


Figure 14: Electronic level structure of the trapped ion. The carrier of the quantum information is the qutrit states $|0\rangle$, $|1\rangle$, and $|2\rangle$.

such as the quantum Fourier transform. Other variations of the ion-trap qutrit quantum computer designs use trapped ions in the presence of a magnetic field gradient [128]. The qutrit ion-trap computer provides a significant increase of the available Hilbert space while demanding only the same amount of physical resources.

4.3 Nuclear magnetic resonance

Nuclear magnetic resonance (NMR) is an essential tool in chemistry and involves manipulating and detecting molecules' nuclear spin states using radio-frequency electromagnetic waves [129]. Some technologies of this field are sophisticated enough to control and observe thousands of nuclei in an experiment. The NMR has the potential to scale up quantum computer to thousands of qudits [130].

In this section we review the implementation of a single-qudit algorithm that can determine the parity of a permutation on an NMR system [15]. The algorithm itself is the parity determining algorithm explained in §3.1.1. The molecule in this NMR setup is embedded in a liquid crystalline environment and the strong magnetic field is used to adjust the anisotropic molecular orientation. This addind a finite quadrupolar coupling term to the Hamiltonian which is as follows

$$H = -\omega_0 I_z + \Lambda(3I_z^2 - I^2), \quad (124)$$

where $\Lambda = e^2 q Q S / 4$ is the effective value of the quadrupolar coupling [15]. The Fourier transformation is implemented by a sequence of three transition-selective pulses, namely,

$$(270)_{x23}(109.47)_{y12}(90)_{y23}. \quad (125)$$

A series of combinations of 180° pulses, both transition-selective and non-selective, is used to implement the permutations.

Final states of the system can be derived from a single projective measurement. Pseudopure spin states act as approximation of effect of the system on an ensemble NMR quantum computer since it is impossible to do the true projective measurements [131]. The fidelity measurement of the experiment is given as

$$F := \frac{\text{tr}(\rho_{\text{th}}^\dagger \rho_{\text{expt}})}{\sqrt{\text{tr}(\rho_{\text{th}}^\dagger \rho_{\text{th}})} \sqrt{\text{tr}(\rho_{\text{expt}}^\dagger \rho_{\text{expt}})}} \quad (126)$$

is used, where ρ_{th} and ρ_{expt} are, respectively, theoretically expected and experimentally obtained density matrices. Fidelities obtained for these proposed operations are 0.92 and above.

Another set-up of the same algorithm treats a single ququart [16]. The algorithm implementation is achieved using a spin $\frac{3}{2}$ nuclei, which is commonly selected for NMR-QIP applications. In their NMR systems the four energy levels needed is made via the Zeeman splitting using a strong static magnetic field. All of the two implementations of the single-qudit algorithm show that the NMR system provides a way to realize a reliable and efficient qudit system for the quantum computing.

4.4 Molecular magnets

Molecular quantum magnets, also called the single-molecule magnets (SMM), provides another physical representation of qudits [119]. They have phenomenal magnetic characteristics and can be manipulated via chemical means. This enables the alternation of the ligand field of the spin carriers and the interaction between the SMM with the other units. As pointed out in one of the proposals, the nuclear spin states of the molecules, which have a long life-time, are used to store the quantum information. This information is read out by the electronic states. In the mean time, the robustness of the molecule allows it to conserve its molecular, electronic and magnetic characteristics at high temperatures [132].

As one of the SMMs, the single molecule TbPc₂ complex reviewed in this section possesses all necessary properties such as long lifetime and robustness. These properties are integrated as important components of a serious quantum mechanical devices, for examples, resonator [133], molecular spin valve [134] and transistor [97, 135]. TbPc₂ gains its SMM properties from the strong spinorbit coupling of lanthanide ions and the ligand field [136]. Magnetic properties of TbPc₂ are governed by the Hamiltonian:

$$\mathcal{H} = \mathcal{H}_f + g_J \mu_0 \mu_B J \cdot H + A_{hf} I \cdot J + (I_z^2 - \frac{1}{3}(I+1)I), \quad (127)$$

where \mathcal{H}_f is the ligand field Hamiltonian, and $g_J \mu_0 \mu_B J \cdot H$ represents the Zeeman energy. $A_{hf} I \cdot J$ accounts for hyperfine interactions and $(I_z^2 - \frac{1}{3}(I+1)I)$ is the quadrupole term. A sweeping magnetic field associated with $m_I = \pm 1/2$ and $\pm 3/2$ can cause quantum tunnelling of magnetisation, which preserves nuclear spin while changing electronic magnetic moment. This field enables nuclear-spin

measurement by suspending the TbPc_2 molecule on carbon nanotubes (CNT) and between gold junctions.

This measurement uses the technique of electro-migration. Initialisation and manipulation of the four spin states of TbPc_2 can be obtained from QTM transitions driven by external ramping magnetic field. The transitions between the $|+1/2\rangle \leftrightarrow |-1/2\rangle$ states and $|+3/2\rangle \leftrightarrow |-3/2\rangle$ is achieved via applying appropriate resonate frequencies ν_{12} and ν_{23} . Relaxation and coherence times are important aspects to be analyzed for the TbPc_2 system, and this process is accomplished by imaging the initialized nuclear spin trajectory in real-time.

Statistical analysis of the nuclear spin coherence time makes use of the spinlattice relaxation times by fitting the data for an exponential form ($y = \exp(-t/T_1)$) and yields $T_1 \approx 17$ s for $m_I = \pm 1/2$ and $T_1 \approx 34$ s for $m_I = \pm 3/2$ with fidelities of $F(m_I = \pm 1/2) \approx 93\%$ and $F(m_I = \pm 3/2) \approx 87\%$ accordingly. [119] The TbPc_2 SMM can be used to execute Grover's algorithm, where the alternation of the m_I state contained in the TbPc_2 molecular qubit are treated by resonance frequencies [17, 137].

5 Summary and future outlook of qudit system

This review article introduces the basics of the high-dimensional qudit systems and provides details about qudit gates, qudit algorithms and implementations on various physical systems. The article serves as a summary of recent developments of qudit quantum computing and an introduction for newcomers to the field of qudit quantum computing. Furthermore we show the advantages and the potential for qudit systems to outperform qubit counterparts.

Qubit algorithms can be generalized and performed with qudits. We have discussed topics concerning qudit gates and algorithms, which form the foundation of gate-based qudit computation and equivalent approaches. Most gates and algorithms based on qudits have some advantage over those for qubits, such as shorter computational time, fewer resources, higher availability, and the ability to solve more complex problems. The qudit system, with its high-dimensional nature, can provide more degrees of freedom and larger computational space. Of course these advantages can come with challenges such as possibly harder-to-implement universal gates, benchmarking [138] and error correction connected with the complexity of the Clifford hierarchy for qudits [44].

Compared to qubit systems, qudit systems currently have received less attention in both theoretical and experimental studies. However, qudit quantum computing is becoming increasingly important as many topics and problems in this field are ripe for exploration. Extending from qubits to qudits ushes in some mathematical challenges, with these mathematical problems elegant and perhaps giving new insights into quantum computing in their own right. Connections between quantum resources such as entanglement, quantum algorithms and their improvements, scaling up qudit systems both to higher dimension and to more particles, benchmarking and error correction, and the bridging between qudits and continuous-variable quantum computing [42] are examples of the fan-

tastic research directions in this field of high-dimensional quantum computing.

Author Contributions

All authors discussed the relevant materials to be added and all participated in writing the article.

Funding

We would like to acknowledge the financial support by the National Science Foundation under award number 1839191-ECCS. BCS appreciates financial support from NSERC and from the Alberta Government.

References

- [1] J.-L. Brylinski and R. Brylinski, “Universal quantum gates,” in *Mathematics of quantum computation*, pp. 117–134, Chapman and Hall/CRC, 2002.
- [2] H.-H. Lu, Z. Hu, M. S. Alshaykh, A. J. Moore, Y. Wang, P. Imany, A. M. Weiner, and S. Kais, “Quantum phase estimation with time-frequency qudits in a single photon,” *Advanced Quantum Technologies*, vol. 0, no. 0, p. 1900074, 2019.
- [3] M. Luo and X. Wang, “Universal quantum computation with qudits,” *Science China Physics, Mechanics & Astronomy*, vol. 57, pp. 1712–1717, Sep 2014.
- [4] B. Li, Z.-H. Yu, and S.-M. Fei, “Geometry of quantum computation with qutrits,” *Sci. Rep.*, vol. 3, p. 2594, 2013.
- [5] M.-X. Luo, X.-B. Chen, Y.-X. Yang, and X. Wang, “Geometry of quantum computation with qudits,” *Sci. Rep.*, vol. 4, p. 4044, 2014.
- [6] V. E. Zobov and A. S. Ermilov, “Implementation of a quantum adiabatic algorithm for factorization on two qudits,” *J. Exp. Theor. Phys.*, vol. 114, pp. 923–932, 07 2012.
- [7] M. H. Amin, N. G. Dickson, and P. Smith, “Adiabatic quantum optimization with qudits,” *Quantum Inf. Process.*, vol. 12, pp. 1819–1829, 04 2013.
- [8] S. X. Cui and Z. Wang, “Universal quantum computation with metaplectic anyons,” *J. Math. Phys.*, vol. 56, no. 3, p. 032202, 2015.
- [9] S. X. Cui, S.-M. Hong, and Z. Wang, “Universal quantum computation with weakly integral anyons,” *Quantum Information Processing*, vol. 14, no. 8, pp. 2687–2727, 2015.
- [10] A. Bocharov, S. X. Cui, M. Roetteler, and K. M. Svore, “Improved quantum ternary arithmetic,” *Quantum Info. Comput.*, vol. 16, p. 862884, July 2016.
- [11] X. Gao, M. Erhard, A. Zeilinger, and M. Krenn, “Computer-inspired concept for high-dimensional multipartite quantum gates,” *arXiv:1910.05677*, 2019.
- [12] S. D. Bartlett, H. de Guise, and B. C. Sanders, “Quantum encodings in spin systems and harmonic oscillators,” *Phys. Rev. A*, vol. 65, p. 052316, May 2002.
- [13] M. R. A. Adcock, P. Høyer, and B. C. Sanders, “Quantum computation with coherent spin states and the close Hadamard problem,” *Quantum Inf. Process.*, vol. 15, pp. 1361–1386, Jan 2016.

- [14] A. B. Klimov, R. Guzmán, J. C. Retamal, and C. Saavedra, “Qutrit quantum computer with trapped ions,” *Phys. Rev. A*, vol. 67, p. 062313, Jun 2003.
- [15] S. Dogra, Arvind, and K. Dorai, “Determining the parity of a permutation using an experimental nmr qutrit,” *Physics Letters A*, vol. 378, no. 46, pp. 3452 – 3456, 2014.
- [16] Z. Gedik, I. A. Silva, B. Lie akmak, G. Karpat, E. L. G. Vidoto, D. O. Soares-Pinto, E. R. deAzevedo, and F. F. Fanchini, “Computational speed-up with a single qudit,” *Sci. Rep.*, vol. 5, pp. 14671 EP –, Oct 2015. Article.
- [17] M. N. Leuenberger and D. Loss, “Quantum computing in molecular magnets,” *Nature*, vol. 410, no. 6830, p. 789, 2001.
- [18] M. Howard and J. Vala, “Qudit versions of the qubit $\pi/8$ gate,” *Phys. Rev. A*, vol. 86, p. 022316, Aug 2012.
- [19] J. Daboul, X. Wang, and B. C. Sanders, “Quantum gates on hybrid qudits,” *J. Phys. A.*, vol. 36, pp. 2525–2536, feb 2003.
- [20] J. C. Garcia-Escartin and P. Chamorro-Posada, “A swap gate for qudits,” *Quantum Inf. Process.*, vol. 12, pp. 3625–3631, Dec 2013.
- [21] T. C. Ralph, K. J. Resch, and A. Gilchrist, “Efficient Toffoli gates using qudits,” *Phys. Rev. A*, vol. 75, p. 022313, Feb 2007.
- [22] E. O. Kiktenko, A. S. Nikolaeva, P. Xu, G. V. Shlyapnikov, and A. K. Fedorov, “Scalable quantum computing with qudits on a graph,” *Phys. Rev. A*, vol. 101, p. 022304, Feb 2020.
- [23] D. M. Nguyen and S. Kim, “Quantum key distribution protocol based on modified generalization of Deutsch-Jozsa algorithm in d-level quantum system,” *International Journal of Theoretical Physics*, vol. 58, pp. 71–82, Jan 2019.
- [24] K. Nagata, H. Geurdes, S. K. Patro, S. Heidari, A. Farouk, and T. Nakamura, “Generalization of the BernsteinVazirani algorithm beyond qubit systems,” *Quantum Stud.: Math. Found.*, vol. 7, pp. 17–21, 03 2020.
- [25] Y. Cao, S.-G. Peng, C. Zheng, and G.-L. Long, “Quantum fourier transform and phase estimation in qudit system,” *Communications in Theoretical Physics*, vol. 55, pp. 790–794, may 2011.
- [26] A. Bocharov, M. Roetteler, and K. M. Svore, “Factoring with qutrits: Shor’s algorithm on ternary and metaplectic quantum architectures,” *Phys. Rev. A*, vol. 96, p. 012306, Jul 2017.

- [27] S. S. Ivanov, H. S. Tonchev, and N. V. Vitanov, “Time-efficient implementation of quantum search with qudits,” *Phys. Rev. A*, vol. 85, p. 062321, Jun 2012.
- [28] A. Y. Vlasov, “Noncommutative tori and universal sets of nonbinary quantum gates,” *J. Math. Phys.*, vol. 43, no. 6, pp. 2959–2964, 2002.
- [29] D. P. DiVincenzo, “Two-bit gates are universal for quantum computation,” *Phys. Rev. A*, vol. 51, no. 2, p. 1015, 1995.
- [30] D. Gottesman, “Fault-tolerant computation with higher-dimensional systems,” in *Lecture Notes in Computer Science* (W. C.P., ed.), vol. 1509 of *NASA International Conference on Quantum Computing and Quantum Communications*, pp. 302–313, Berlin: Springer, 1999.
- [31] D. L. Zhou, B. Zeng, Z. Xu, and C. P. Sun, “Quantum computation based on d -level cluster state,” *Phys. Rev. A*, vol. 68, p. 062303, Dec 2003.
- [32] S. S. Bullock, D. P. O’Leary, and G. K. Brennen, “Asymptotically optimal quantum circuits for d -level systems,” *Phys. Rev. Lett.*, vol. 94, p. 230502, Jun 2005.
- [33] W.-D. Li, Y.-J. Gu, K. Liu, Y.-H. Lee, and Y.-Z. Zhang, “Efficient universal quantum computation with auxiliary Hilbert space,” *Phys. Rev. A*, vol. 88, p. 034303, Sep 2013.
- [34] B. Mischuck and K. Mølmer, “Qudit quantum computation in the Jaynes-Cummings model,” *Phys. Rev. A*, vol. 87, p. 022341, Feb 2013.
- [35] M. Reck, A. Zeilinger, H. J. Bernstein, and P. Bertani, “Experimental realization of any discrete unitary operator,” *Phys. Rev. Lett.*, vol. 73, pp. 58–61, Jul 1994.
- [36] D. J. Rowe, B. C. Sanders, and H. de Guise, “Representations of the Weyl group and Wigner functions for $SU(3)$,” *J. Math. Phys.*, vol. 40, no. 7, pp. 3604–3615, 1999.
- [37] A. Muthukrishnan and C. R. Stroud, “Multivalued logic gates for quantum computation,” *Phys. Rev. A*, vol. 62, p. 052309, Oct 2000.
- [38] G. K. Brennen, D. P. O’Leary, and S. S. Bullock, “Criteria for exact qudit universality,” *Phys. Rev. A*, vol. 71, p. 052318, May 2005.
- [39] D. Gottesman, “Theory of fault-tolerant quantum computation,” *Phys. Rev. A*, vol. 57, pp. 127–137, Jan 1998.
- [40] P. Boykin, T. Mor, M. Pulver, V. Roychowdhury, and F. Vatan, “A new universal and fault-tolerant quantum basis,” *Information Processing Letters*, vol. 75, no. 3, pp. 101 – 107, 2000.

- [41] J. Patera and H. Zassenhaus, “The Pauli matrices in n dimensions and finest gradings of simple lie algebras of type A_{n-1} ,” *J. Math. Phys.*, vol. 29, no. 3, pp. 665–673, 1988.
- [42] D. Gottesman, A. Kitaev, and J. Preskill, “Encoding a qubit in an oscillator,” *Phys. Rev. A*, vol. 64, no. 1, p. 012310, 2001.
- [43] M. A. Nielsen, M. J. Bremner, J. L. Dodd, A. M. Childs, and C. M. Dawson, “Universal simulation of hamiltonian dynamics for quantum systems with finite-dimensional state spaces,” *Phys. Rev. A*, vol. 66, p. 022317, Aug 2002.
- [44] Z. Webb, “The Clifford group forms a unitary 3-design,” *Quantum Inf. Comput.*, vol. 16, no. 15&16, pp. 1379–1400, 2016.
- [45] D. Gottesman and I. L. Chuang, “Demonstrating the viability of universal quantum computation using teleportation and single-qubit operations,” *Nature*, vol. 402, no. 6760, pp. 390–393, 1999.
- [46] B. Eastin and E. Knill, “Restrictions on transversal encoded quantum gate sets,” *Phys. Rev. Lett.*, vol. 102, p. 110502, Mar 2009.
- [47] B. Zeng, H. Chung, A. W. Cross, and I. L. Chuang, “Local unitary versus local Clifford equivalence of stabilizer and graph states,” *Phys. Rev. A*, vol. 75, p. 032325, Mar 2007.
- [48] R. A. Low, “Learning and testing algorithms for the Clifford group,” *Phys. Rev. A*, vol. 80, p. 052314, Nov 2009.
- [49] A. M. Childs, “Secure assisted quantum computation,” *arXiv:quant-ph/0111046*, 2001.
- [50] W. van Dam and M. Howard, “Noise thresholds for higher-dimensional systems using the discrete wigner function,” *Phys. Rev. A*, vol. 83, p. 032310, Mar 2011.
- [51] H. Anwar, E. T. Campbell, and D. E. Browne, “Qutrit magic state distillation,” *New Journal of Physics*, vol. 14, p. 063006, jun 2012.
- [52] E. T. Campbell, H. Anwar, and D. E. Browne, “Magic-state distillation in all prime dimensions using quantum Reed-Muller codes,” *Phys. Rev. X*, vol. 2, p. 041021, Dec 2012.
- [53] C. M. Wilmott, “On swapping the states of two qudits,” *Int. J. Quantum Inf.*, vol. 09, no. 06, pp. 1511–1517, 2011.
- [54] C. M. Wilmott and P. R. Wild, “On a generalized quantum swap gate,” *Int. J. Quantum Inf.*, vol. 10, no. 03, p. 1250034, 2012.
- [55] N. D. Mermin, “From classical state swapping to quantum teleportation,” *Phys. Rev. A*, vol. 65, p. 012320, Dec 2001.

- [56] K. Fujii, “Exchange gate on the qudit space and fock space,” *J. Opt. B*, vol. 5, pp. S613–S618, oct 2003.
- [57] G. A. Paz-Silva, S. Rebić, J. Twamley, and T. Duty, “Perfect mirror transport protocol with higher dimensional quantum chains,” *Phys. Rev. Lett.*, vol. 102, p. 020503, Jan 2009.
- [58] X. Wang, “Continuous-variable and hybrid quantum gates,” *J. Phys. A*, vol. 34, pp. 9577–9584, oct 2001.
- [59] G. Alber, A. Delgado, N. Gisin, and I. Jex, “Efficient bipartite quantum state purification in arbitrary dimensional Hilbert spaces,” *J. Phys. A*, vol. 34, pp. 8821–8833, oct 2001.
- [60] A. M. C. R. Stroud, “Quantum fast fourier transform using multilevel atoms,” *J. Mod. Opt.*, vol. 49, no. 13, pp. 2115–2127, 2002.
- [61] D. G. Cory, M. D. Price, W. Maas, E. Knill, R. Laflamme, W. H. Zurek, T. F. Havel, and S. S. Somaroo, “Experimental quantum error correction,” *Phys. Rev. Lett.*, vol. 81, pp. 2152–2155, Sep 1998.
- [62] E. Dennis, “Toward fault-tolerant quantum computation without concatenation,” *Phys. Rev. A*, vol. 63, p. 052314, Apr 2001.
- [63] Y. Shi, “Both Toffoli and controlled-NOT need little help to do universal quantum computation,” *arXiv preprint quant-ph/0205115*, 2002.
- [64] M. A. Nielsen and I. L. Chuang, *Quantum Computation and Quantum Information: 10th Anniversary Edition*. New York, NY, USA: Cambridge University Press, 10th ed., 2011.
- [65] A. Aspuru-Guzik, A. D. Dutoi, P. J. Love, and M. Head-Gordon, “Simulated quantum computation of molecular energies,” *Science*, vol. 309, no. 5741, pp. 1704–1707, 2005.
- [66] P. W. Shor, “Algorithms for quantum computation: discrete logarithms and factoring,” in *Proceedings 35th Annual Symposium on Foundations of Computer Science*, pp. 124–134, Nov 1994.
- [67] R. Cleve, A. Ekert, C. Macchiavello, and M. Mosca, “Quantum algorithms revisited,” *Proceedings of the Royal Society of London. Series A: Mathematical, Physical and Engineering Sciences*, vol. 454, no. 1969, pp. 339–354, 1998.
- [68] Y.-M. Di and H.-R. Wei, “Synthesis of multivalued quantum logic circuits by elementary gates,” *Phys. Rev. A*, vol. 87, p. 012325, Jan 2013.
- [69] F. S. Khan and M. Perkowski, “Synthesis of multi-qudit hybrid and d-valued quantum logic circuits by decomposition,” *Theor. Comput. Sci.*, vol. 367, no. 3, pp. 336 – 346, 2006.

- [70] M. A. Nielsen, M. R. Dowling, M. Gu, and A. C. Doherty, “Quantum computation as geometry,” *Science*, vol. 311, no. 5764, pp. 1133–1135, 2006.
- [71] M. A. Nielsen, “A geometric approach to quantum circuit lower bounds,” *arXiv preprint quant-ph/0502070*, 2005.
- [72] D. Deutsch, “Quantum theory, the Church–Turing principle and the universal quantum computer,” *J. Phys. A*, vol. 400, no. 1818, pp. 97–117, 1985.
- [73] D. P. Deutsch and R. Jozsa, “Rapid solution of problems by quantum computation,” *Proc. Royal Soc. Lond. A*, vol. 439, pp. 553–558, 1992.
- [74] M. Van den Nest, “Universal quantum computation with little entanglement,” *Phys. Rev. Lett.*, vol. 110, p. 060504, Feb 2013.
- [75] M. Howard, J. Wallman, V. Veitch, and J. Emerson, “Contextuality supplies the ‘magic’ for quantum computation,” *Nature*, vol. 510, p. 351, Jun 2014. Article.
- [76] S. Kochen and E. P. Specker, *The Problem of Hidden Variables in Quantum Mechanics*, pp. 293–328. Dordrecht: Springer Netherlands, 1975.
- [77] A. A. Klyachko, M. A. Can, S. Binicioğlu, and A. S. Shumovsky, “Simple test for hidden variables in spin-1 systems,” *Phys. Rev. Lett.*, vol. 101, p. 020403, Jul 2008.
- [78] X. Zhan, J. Li, H. Qin, Z. hao Bian, and P. Xue, “Linear optical demonstration of quantum speed-up with a single qudit,” *Opt. Express*, vol. 23, pp. 18422–18427, Jul 2015.
- [79] Y. Fan, “A generalization of the Deutsch-Jozsa algorithm to multi-valued quantum logic,” in *37th International Symposium on Multiple-Valued Logic (ISMVL’07)*, pp. 12–12, May 2007.
- [80] E. Kiktenko, A. Fedorov, A. Strakhov, and V. Man’ko, “Single qudit realization of the Deutsch algorithm using superconducting many-level quantum circuits,” *Physics Letters A*, vol. 379, no. 22, pp. 1409 – 1413, 2015.
- [81] A. R. Kessel and N. M. Yakovleva, “Implementation schemes in NMR of quantum processors and the Deutsch-Jozsa algorithm by using virtual spin representation,” *Phys. Rev. A*, vol. 66, p. 062322, Dec 2002.
- [82] E. Bernstein and U. Vazirani, “Quantum complexity theory,” *SIAM Journal on Computing*, vol. 26, no. 5, pp. 1411–1473, 1997.
- [83] R. Krishna, V. Makwana, and A. P. Suresh, “A generalization of Bernstein-Vazirani algorithm to qudit systems,” *arXiv preprint arXiv:1609.03185*, 2016.

- [84] Z. Zilic and K. Radecka, “Scaling and better approximating quantum Fourier transform by higher radices,” *IEEE Transactions on Computers*, vol. 56, pp. 202–207, Feb 2007.
- [85] D. Coppersmith, “An approximate Fourier transform useful in quantum factoring,” *arXiv preprint quant-ph/0201067*, 2002.
- [86] V. V. Shende, S. S. Bullock, and I. L. Markov, “Synthesis of quantum-logic circuits,” *IEEE Transactions on Computer-Aided Design of Integrated Circuits and Systems*, vol. 25, pp. 1000–1010, June 2006.
- [87] V. Parasa and M. Perkowski, “Quantum phase estimation using multi-valued logic,” in *2011 41st IEEE International Symposium on Multiple-Valued Logic*, pp. 224–229, May 2011.
- [88] D. S. Abrams and S. Lloyd, “Quantum algorithm providing exponential speed increase for finding eigenvalues and eigenvectors,” *Phys. Rev. Lett.*, vol. 83, pp. 5162–5165, Dec 1999.
- [89] A. W. Harrow, A. Hassidim, and S. Lloyd, “Quantum algorithm for linear systems of equations,” *Phys. Rev. Lett.*, vol. 103, p. 150502, Oct 2009.
- [90] J. Pan, Y. Cao, X. Yao, Z. Li, C. Ju, H. Chen, X. Peng, S. Kais, and J. Du, “Experimental realization of quantum algorithm for solving linear systems of equations,” *Physical Review A*, vol. 89, no. 2, p. 022313, 2014.
- [91] H. S. Tonchev and N. V. Vitanov, “Quantum phase estimation and quantum counting with qudits,” *Phys. Rev. A*, vol. 94, p. 042307, Oct 2016.
- [92] H. Wang, S. Kais, A. Aspuru-Guzik, and M. R. Hoffmann, “Quantum algorithm for obtaining the energy spectrum of molecular systems,” *Phys. Chem. Chem. Phys.*, vol. 10, pp. 5388–5393, 2008.
- [93] A. Daskin and S. Kais, “Decomposition of unitary matrices for finding quantum circuits: application to molecular hamiltonians,” *The Journal of chemical physics*, vol. 134, no. 14, p. 144112, 2011.
- [94] A. Daskin, A. Grama, G. Kollias, and S. Kais, “Universal programmable quantum circuit schemes to emulate an operator,” *The Journal of chemical physics*, vol. 137, no. 23, p. 234112, 2012.
- [95] S. Kais, “Introduction to quantum information and computation for chemistry,” *Quantum Inf. Comput. Chem.*, vol. 154, pp. 1–38, 2014.
- [96] T. Bian, D. Murphy, R. Xia, A. Daskin, and S. Kais, “Quantum computing methods for electronic states of the water molecule,” *Molecular Physics*, vol. 117, no. 15-16, pp. 2069–2082, 2019.
- [97] M. Sawerwain and W. Leoński, “Quantum circuits based on qutrits as a tool for solving systems of linear equations,” *arXiv:1309.0800*, 2013.

- [98] P. W. Shor, “Polynomial-time algorithms for prime factorization and discrete logarithms on a quantum computer,” *SIAM review*, vol. 41, no. 2, pp. 303–332, 1999.
- [99] Y. Fan, “Applications of multi-valued quantum algorithms,” *arXiv:0809.0932*, 2008.
- [100] H. Li, C. Wu, W. Liu, P. Chen, and C. Li, “Fast quantum search algorithm for databases of arbitrary size and its implementation in a cavity QED system,” *Physics Letters A*, vol. 375, no. 48, pp. 4249 – 4254, 2011.
- [101] E. S. Kyoseva and N. V. Vitanov, “Coherent pulsed excitation of degenerate multistate systems: Exact analytic solutions,” *Phys. Rev. A*, vol. 73, p. 023420, Feb 2006.
- [102] F. Jelezko, T. Gaebel, I. Popa, M. Domhan, A. Gruber, and J. Wrachtrup, “Observation of coherent oscillation of a single nuclear spin and realization of a two-qubit conditional quantum gate,” *Phys. Rev. Lett.*, vol. 93, p. 130501, Sep 2004.
- [103] L. Childress, M. V. Gurudev Dutt, J. M. Taylor, A. S. Zibrov, F. Jelezko, J. Wrachtrup, P. R. Hemmer, and M. D. Lukin, “Coherent dynamics of coupled electron and nuclear spin qubits in diamond,” *Science*, vol. 314, no. 5797, pp. 281–285, 2006.
- [104] P. Neumann, J. Beck, M. Steiner, F. Rempp, H. Fedder, P. R. Hemmer, J. Wrachtrup, and F. Jelezko, “Single-shot readout of a single nuclear spin,” *Science*, vol. 329, no. 5991, pp. 542–544, 2010.
- [105] D. Loss and D. P. DiVincenzo, “Quantum computation with quantum dots,” *Phys. Rev. A*, vol. 57, pp. 120–126, Jan 1998.
- [106] K. C. Nowack, F. H. L. Koppens, Y. V. Nazarov, and L. M. K. Vandersypen, “Coherent control of a single electron spin with electric fields,” *Science*, vol. 318, no. 5855, pp. 1430–1433, 2007.
- [107] G. J. Milburn, “Photons as qubits,” *Physica Scripta*, vol. T137, p. 014003, dec 2009.
- [108] R. Prevedel, P. Walther, F. Tiefenbacher, P. BMei hi, R. Kaltenbaek, T. Jennewein, and A. Zeilinger, “High-speed linear optics quantum computing using active feed-forward,” *Nature*, vol. 445, no. 7123, pp. 65–69, 2007.
- [109] I. Chiorescu, Y. Nakamura, C. J. P. M. Harmans, and J. E. Mooij, “Coherent quantum dynamics of a superconducting flux qubit,” *Science*, vol. 299, no. 5614, pp. 1869–1871, 2003.
- [110] J. Clarke and F. K. Wilhelm, “Superconducting quantum bits,” *Nature*, vol. 453, no. 7198, pp. 1031–1042, 2008.

- [111] R. Blatt and D. Wineland, “Entangled states of trapped atomic ions,” *Nature*, vol. 453, no. 7198, pp. 1008–1015, 2008.
- [112] I. Bloch, “Quantum coherence and entanglement with ultracold atoms in optical lattices,” *Nature*, vol. 453, no. 7198, pp. 1016–1022, 2008.
- [113] F. Troiani and M. Affronte, “Molecular spins for quantum information technologies,” *Chemical Society Reviews*, vol. 40, no. 6, pp. 3119–3129, 2011.
- [114] L. Bogani and W. Wernsdorfer, “Molecular spintronics using single-molecule magnets,” in *Nanoscience And Technology: A Collection of Reviews from Nature Journals*, pp. 194–201, World Scientific, 2010.
- [115] J. M. Clemente-Juan, E. Coronado, and A. Gaita-Ariño, “Magnetic polyoxometalates: from molecular magnetism to molecular spintronics and quantum computing,” *Chemical Society Reviews*, vol. 41, no. 22, pp. 7464–7478, 2012.
- [116] G. Aromí, D. Aguila, P. Gamez, F. Luis, and O. Roubeau, “Design of magnetic coordination complexes for quantum computing,” *Chemical Society Reviews*, vol. 41, no. 2, pp. 537–546, 2012.
- [117] I. L. Chuang, L. M. Vandersypen, X. Zhou, D. W. Leung, and S. Lloyd, “Experimental realization of a quantum algorithm,” *Nature*, vol. 393, no. 6681, p. 143, 1998.
- [118] L. M. Vandersypen, M. Steffen, G. Breyta, C. S. Yannoni, M. H. Sherwood, and I. L. Chuang, “Experimental realization of Shor’s quantum factoring algorithm using nuclear magnetic resonance,” *Nature*, vol. 414, no. 6866, p. 883, 2001.
- [119] E. Moreno-Pineda, C. Godfrin, F. Balestro, W. Wernsdorfer, and M. Ruben, “Molecular spin qubits for quantum algorithms,” *Chem. Soc. Rev.*, vol. 47, pp. 501–513, 2018.
- [120] A. Babazadeh, M. Erhard, F. Wang, M. Malik, R. Nouroozi, M. Krenn, and A. Zeilinger, “High-dimensional single-photon quantum gates: Concepts and experiments,” *Phys. Rev. Lett.*, vol. 119, p. 180510, Nov 2017.
- [121] M. Erhard, R. Fickler, M. Krenn, and A. Zeilinger, “Twisted photons: new quantum perspectives in high dimensions,” *Light Sci. Appl.*, vol. 7, p. 17146, 2018.
- [122] M. Kues, C. Reimer, P. Roztocky, L. Romero Corts, S. Sciara, B. Wetzell, Y. Zhang, A. Cino, S. T. Chu, B. E. Little, D. J. Moss, L. Caspani, J. Azaña, and R. Morandotti, “On-chip generation of high-dimensional entangled quantum states and their coherent control,” *Nature*, vol. 546, no. 6760, pp. 622–626, 2017.

- [123] H.-H. Lu, J. M. Lukens, N. A. Peters, O. D. Odele, D. E. Leaird, A. M. Weiner, and P. Lougovski, “Electro-optic frequency beam splitters and tritters for high-fidelity photonic quantum inf. process.,” *Phys. Rev. Lett.*, vol. 120, no. 3, p. 030502, 2018.
- [124] P. Imany, J. A. Jaramillo-Villegas, O. D. Odele, K. Han, D. E. Leaird, J. M. Lukens, P. Lougovski, M. Qi, and A. M. Weiner, “50-ghz-spaced comb of high-dimensional frequency-bin entangled photons from an on-chip silicon nitride microresonator,” *Opt. Express*, vol. 26, no. 2, pp. 1825–1840, 2018.
- [125] P. Imany, J. A. Jaramillo-Villegas, M. S. Alshaykh, J. M. Lukens, O. D. Odele, A. J. Moore, D. E. Leaird, M. Qi, and A. M. Weiner, “High-dimensional optical quantum logic in large operational spaces,” *npj Quantum Inf.*, vol. 5, Jul 2019.
- [126] N. T. Islam, C. C. W. Lim, C. Cahall, J. Kim, and D. J. Gauthier, “Probably secure and high-rate quantum key distribution with time-bin qudits,” *Science advances*, vol. 3, no. 11, p. e1701491, 2017.
- [127] P. C. Humphreys, B. J. Metcalf, J. B. Spring, M. Moore, X.-M. Jin, M. Barbieri, W. S. Kolthammer, and I. A. Walmsley, “Linear optical quantum computing in a single spatial mode,” *Phys. Rev. Lett.*, vol. 111, p. 150501, Oct 2013.
- [128] D. Mc Hugh and J. Twamley, “Trapped-ion qutrit spin molecule quantum computer,” *New J. Phys.*, vol. 7, no. 1, p. 174, 2005.
- [129] F. A. Bovey, P. A. Mirau, and H. Gutowsky, *Nuclear magnetic resonance spectroscopy*. Elsevier, 1988.
- [130] C. P. Slichter, *Principles of magnetic resonance*, vol. 1. Springer Science & Business Media, 2013.
- [131] J.-S. Lee and A. K. Khitrin, “Projective measurement in nuclear magnetic resonance,” *Applied physics letters*, vol. 89, no. 7, p. 074105, 2006.
- [132] E. Moreno Pineda, T. Komeda, K. Katoh, M. Yamashita, and M. Ruben, “Surface confinement of TbPc2-SMMs: structural, electronic and magnetic properties,” *Dalton Trans.*, vol. 45, pp. 18417–18433, 2016.
- [133] M. Ganzhorn, S. Klyatskaya, M. Ruben, and W. Wernsdorfer, “Strong spin–phonon coupling between a single-molecule magnet and a carbon nanotube nanoelectromechanical system,” *Nat. Nanotechnol.*, vol. 8, no. 3, p. 165, 2013.
- [134] M. Urdampilleta, S. Klyatskaya, J.-P. Cleuziou, M. Ruben, and W. Wernsdorfer, “Supramolecular spin valves,” *Nature materials*, vol. 10, no. 7, p. 502, 2011.

- [135] S. Thiele, F. Balestro, R. Ballou, S. Klyatskaya, M. Ruben, and W. Wernsdorfer, “Electrically driven nuclear spin resonance in single-molecule magnets,” *Science*, vol. 344, no. 6188, pp. 1135–1138, 2014.
- [136] N. Ishikawa, M. Sugita, T. Okubo, N. Tanaka, T. Iino, and Y. Kaizu, “Determination of ligand-field parameters and f-electronic structures of double-decker bis (phthalocyaninato) lanthanide complexes,” *Inorganic chemistry*, vol. 42, no. 7, pp. 2440–2446, 2003.
- [137] C. Godfrin, A. Ferhat, R. Ballou, S. Klyatskaya, M. Ruben, W. Wernsdorfer, and F. Balestro, “Operating quantum states in single magnetic molecules: implementation of grovers quantum algorithm,” *Phys. Rev. Lett.*, vol. 119, no. 18, p. 187702, 2017.
- [138] M. Jafarzadeh, Y.-D. Wu, Y. R. Sanders, and B. C. Sanders, “Randomized benchmarking for qudit Clifford gates,” *New J. Phys.*, vol. 22, p. 063014, 06 2020.